

Some Properties of Thin Beds

H. Chung and D. Lawton

ABSTRACT

Six thin-bed models as represented by six two-termed reflectivity series are convolved with a Ricker 31 Hz zero-phase wavelet. The absolute maximum amplitude (AMA) and the peak frequency (PF) of the resultant composite wavelet are studied. It is found that for unequal polarity, the AMA increases with thickness, and vice versa for equal polarity in the range of thickness between one-eighth and one-quarter of the predominant wavelength. The functional dependence is, in general, nonlinear, except in the case of unequal polarity and equal strength. The PF decreases quadratically as a function of thickness for the equal polarity models. For the unequal polarity models, it first increases with thickness and then decreases. But for the unequal polarity and equal strength model (Widess' model, 1973), the PF of the composite wavelet is found to be $\sqrt{3}/2f_0$ for thickness for which the thin-bed assumption is valid, where f_0 is the PF of the input wavelet. Mathematical expressions for the AMA and the PF have also been derived. To study the phase, complex attributes are used. However, the results are not conclusive and more study is needed.

INTRODUCTION

In the Western Canadian Sedimentary Basin, the geological formations comprising the Cretaceous period are composed of many thin clastic layers such as interbedded sandstones and shales. Many of these layers have thicknesses below the vertical resolution limit with respect to the frequencies common on seismic data. A good example is the Bluesky Formation in the Waskahigan area of West Central Alberta, where its thickness rarely exceeds 10 m. With a P-wave velocity of about 4600 m/sec and a peak frequency of 35 Hz, its resolution limit, which is a quarter of the predominant wavelength, is 25 m. Hence, one cannot possibly resolve the top and bottom interfaces of the formation. Under these circumstances, stratigraphic interpretation is employed where amplitude information is used to deduce the thickness and lithology of the thin bed.

The purpose of our study is to investigate effective ways of delineating thin beds. While this paper deals only with the properties of a single thin bed, our next step will be to expand our investigation into the properties of a wavelet which is a composite reflection of two and three thin layers. Our ultimate objective is to develop some algorithm to delineate thin beds, using existing tools such as AVO analysis and complex attributes.

This paper deals only with vertical incidence, and the emphasis will be on bed thicknesses that are below the resolution limit. Two-termed reflectivity series of equal and unequal strengths with both equal and opposite polarities will be studied.

BACKGROUND

Many authors have discussed the responses of thin beds to vertically incident plane wave. Widess (1973) considered a homogeneous thin layer embedded in an infinite homogeneous medium with higher velocity. He concluded that when the bed thins to one-eighth of the predominant wavelength, the reflected wavelet would assume the form of the derivative of the input zero-phase wavelet. He also proposed (1982) to use Am^2/E as a quantitative measure of resolving power for the composite wavelet, where Am is the maximum amplitude of the wavelet, and E is the total energy of the wavelet. Neidell and Poggiagliolmi (1977) emphasized the use of reflection amplitudes and waveforms for quantitatively analyzing thin beds of spatial extent that were small compared to the corresponding Fresnel zone. Koefoed and de Voogd (1980) studied the linear properties of thin layers for the thickness range below the resolution limit. Various authors have used different criteria to define the resolution limit of thin beds, but Kalweit and Wood (1982) showed that Ricker's (1953) zero-curvature criterion for temporal resolution could be generalized to the two-termed reflectivity series of equal strength and opposite polarity as well as to the case of equal strength and equal polarity. De Voogd and den Rooijen (1983) derived quantitatively the response of a thin layer to a vertically incident seismic pulse, and concluded that the reflected pulse had the shape of the time derivative of the incident wavelet, and its amplitude proportional to the two-way travel time in the thin layer.

To study the responses of a single thin bed to a vertically incident plane wave, a simple wedge model (Fig. 1) is used. All the model synthetic seismograms are generated by convolving a zero-phase 31 Hz Ricker wavelet with various two-terms reflectivity series. Note that a zero-phase wavelet gives the maximum vertical resolution compared to other phases (Berkout, 1984). Six different two-terms reflectivity series will be studied:

- (a) \uparrow , opposite polarity and equal strength
- (b) \downarrow , opposite polarity and unequal strength
- (c) \uparrow , opposite polarity and unequal strength
- (d) \uparrow , equal polarity and equal strength
- (e) \downarrow , equal polarity and unequal strength
- (f) \uparrow , equal polarity and unequal strength

The densities and velocities used for the various models are listed in Table 1. They are chosen to reflect the general situation in the early Cretaceous formations in Southern Alberta. Figure 2 shows the synthetic seismograms for the six models. Recall that our zone of interest is in the thickness range below tuning, i.e. below the thickness equal to one-quarter of the predominant wavelength for all the models. For the equal polarity cases, at thicknesses below one-eighth of the predominant wavelength, the reflected composite wavelet appears to be zero-phase for all three cases. It is about half-way between the one-eighth and one-quarter limit that the phase of the wavelet starts to appear differently among the three cases. Furthermore, the maximum amplitude of the wavelet for all three cases decreases with thickness.

For the unequal polarity cases, the maximum amplitude increases with thickness for all the three models. However, the wavelet in model 1A clearly resembles a 90 phase wavelet below the thickness of one-eighth of the predominant wavelength, but for models 1C and 1B, it resembles a zero-phase wavelet in the former and an inverted zero-phase wavelet in the latter for thicknesses below five meters, which is about one-sixteenth of the predominant wavelength. This difference in phase can be used to infer whether we have similar half-spaces or dissimilar half-spaces above and below the thin bed. This result is also reported by Lange and Almoghrabi (1988).

We shall further discuss the amplitude, frequency and phase separately. Throughout the whole paper, the term 'thickness of interest' will be used repeatedly. It refers to the thickness range between zero and a quarter of the predominant wavelength.

AMPLITUDE

Of the three attributes of a reflected wavelet, namely, amplitude, frequency, and phase, the amplitude is the most studied one for thin bed interpretation. Various authors (Widess, 1973; Neidell and Poggialiomi, 1977; Koefoed and de Voogd, 1980; Kalweit and Wood, 1982; De Voogd and den Rooijen, 1983) have discussed the relationship between the amplitude of the reflected composite wavelet and the thickness of the bed. In particular, Widess (1973) and De Voogd and den Rooijen (1983) have both developed mathematical expressions which relate the maximum amplitude response of a homogeneous thin bed imbedded in a thick homogeneous bed to vertically incident plane waves. While Widess ignored transmission loss and internal multiple, and De Voogd and den Rooijen considered them, they both concluded that the maximum amplitude is linearly proportional to both the bed thickness and the reflection coefficient and is inversely proportional to the incident predominant wavelength. But their conclusion is limited only to the case represented by model 1A, i.e. opposite polarity and equal strength.

In Appendix A, we derive a mathematical expression which relates the absolute maximum amplitude response of a thin bed to the thickness of the bed for the general case. The result is:

$$\phi_{\text{abs. max}} = \left\{ (r_1 + r_2)^2 \left[1 - 2 \left(\frac{\pi b}{\lambda_d} \right)^2 \right]^2 + (r_2 - r_1)^2 \left(\frac{2\pi b}{\lambda_d} \right)^2 \right\}^{1/2} \quad (\text{I})$$

where $\phi_{\text{abs.max}}$ = absolute maximum amplitude of reflected composite wavelet/absolute maximum amplitude of incident wavelet

r_1 = reflection coefficient of upper interface

r_2 = reflection coefficient of lower interface

b = thin bed thickness

= predominant wavelength of the input wavelet

Note that in deriving equation (I), transmission loss and internal multiples are ignored. As pointed out by Koefoed and de Voogd (1980), such effects are negligible as long as the acoustic impedance ratio between the thin layer and the surrounding rock lies between the bounds of 0.5 and 2, which they also pointed out is the range of acoustic contrast usually encountered in practice.

Equation (I) gives the absolute maximum amplitude response of a thin bed for the general case. The first term within the bracket disappears for $r_1 = -r_2$, and the second term becomes $4\pi r_1 b / \lambda_d$, which is the expression derived by Widess (1973). For $r_1 = r_2$, the second term becomes zero and the first term $2r_1[1 - 2\pi^2 b^2 / \lambda_d^2]$, which gives a value of $\phi_{\text{abs.max}} = 2r_1$ for $b = 0$ as expected. The expression for $\phi_{\text{abs.max}}$ also indicates that, except for the case where $r_1 = -r_2$, the absolute maximum amplitude of a composite wavelet reflected from a thin bed is not linearly proportional to the bed thickness, but rather, the relationship is a complicated second-ordered polynomial. This implies that on exploration seismic data, calibration of amplitude to infer thickness based on a linear relationship will lead to erroneous results unless $r_2 = -r_1$.

Figure 3 shows the plots of amplitude versus thickness for the six models. Both the maximum peaks and minimum troughs are plotted. For all cases, the tuning thickness is at one-quarter of the predominant wavelength, and is a maximum for the unequal polarity models and a minimum for the equal polarity models. The slightly off-maximum and off-minimum positions for some of the one-quarter predominant wavelength arrow indicators are probably due to round-off error in the modelling package.

For the equal polarity cases, the agreement between the theoretical and modelling results is good up to a thickness about two meters below the one-eighth of the predominant wavelength. Note also that the profile of the peak curves and trough curves for models 1E and 1F are very similar, and if one plots the peak to trough ratios for these two models, the resulting two curves would be quite similar. But model 1D shows a more rapidly decreasing peak curve, so that a peak to trough ratio curve would decrease with thickness faster than the ones for unequal strengths.

For the unequal polarity, the results for model 1A has been studied thoroughly by many authors. As expected, tuning occurs at the thickness equal to one-quarter of the predominant wavelength, and the linearity limit for the maximum amplitude versus thickness relationship ends at a thickness slightly greater than one-eighth of the predominant wavelength. The peak to trough ratio is also close to unity. But for the unequal strengths models 1B and 1C, the results are significantly different. Note that the peak and trough amplitudes for model 1B are equal to the trough and peak amplitudes respectively for 1C. This is because r_1 and r_2 for model 1B are equal to r_2 and r_1 respectively for model 1C. Hence, the peak to trough ratios for the two models are reciprocals, and are obviously not equal to unity. The theoretical curve agrees with the models only up to about five meters, which is about one-sixteenth of the predominant wavelength. The reason for this lower agreement limit compared to model 1A is not well understood at present. We will test equation (I) further with various parameters. In particular, we will test it against physical modelling results.

FREQUENCY

The relationship of peak frequency versus thickness for a thin bed has not been studied extensively in published literature. Lange and Almoghrabi (1988) studied the peak frequency as a function of both offset and thickness for opposite polarities of both equal and unequal strengths. They showed that the peak frequency first increases with the thickness for small thicknesses, and decreases as the thickness continues to increase. The exact behavior is dependent on the reflection coefficients of both upper and lower interfaces. But their study is based on modelling results. We now present mathematical expressions relating the peak frequency to the thickness of the thin bed. The derivations are shown in Appendix B.

The equation relating the peak frequency to the bed thickness is:

$$f_p \left[r_1 r_2 \pi \Delta T \sin(2\pi f_p \Delta T) \right] = \left[r_1^2 + r_2^2 + 2r_1 r_2 \cos(2\pi f_p \Delta T) \right] \left[1 - \left(\frac{f_p}{f_0} \right)^2 \right] \quad (\text{II})$$

where r_1 = reflection coefficient of the upper interface
 r_2 = reflection coefficient of the lower interface
 f_p = peak frequency of reflected composite wavelet
 ΔT = 2-way travel time in the thin layer
 $= 2 \times \frac{\text{bed thickness}}{\text{P-wave velocity in the bed}}$
 f_0 = peak frequency of the input wavelet

Note that equation (II) is an exact equation in that no approximation has been taken (Appendix B). It is only valid for Ricker zero-phase wavelets. If we make the thin bed assumption (Appendix B), it reduces to

$$f_p \approx f_0 \left[1 - \frac{\pi^2 \Delta T^2 f_0^2 r_1 r_2}{k} \right] \quad \text{where } k = r_1^2 + r_2^2 + 2r_1 r_2 = (r_1 + r_2)^2 \quad (\text{III})$$

Equation (III) may be considered as the equation that governs the relationship between the peak frequency of the reflected composite wavelet from a thin bed and the bed thickness for all cases except when $r_1 = -r_2$. It indicates that for opposite polarity cases, the peak frequency increases as the bed thickness increases, and vice versa for equal polarity. But equation (III) will not be valid at thicknesses beyond the thin bed limit inherent in the thin bed assumption (Appendix B). For $r_1 = -r_2$, the fraction within the bracket in equation (III) will become infinity and hence equation (III) cannot be used for this case. However, as Appendix B illustrates, a different approach of approximation can be taken with equation (II) to accommodate the case of $r_1 = -r_2$. The result is that the peak frequency f_p is given by:

$$f_p = \sqrt{\frac{3}{2}} f_0$$

This result obviously only holds for thicknesses for which the thin bed approximation is valid. But this result is a very interesting one. Widess (1973) showed that for $r_1 = -r_2$, when the thickness is at one-eighth of the predominant wavelength, the reflected composite wavelet assumes the form of the derivative of the incident wavelet. But his conclusion is graphical. Lange and Almoghrabi (1988) showed quantitatively that, assuming Widess' conclusion is correct, one would obtain a new peak frequency given by $f_p = \sqrt{3/2}f_o$. Hence, combining their results, with the calculation in Appendix B for $r_1 = -r_2$, Widess' conclusion is confirmed quantitatively.

Figure 4 shows the plots of the peak frequency versus the thickness for the six models. For the equal polarity cases, the modelling results and the theoretical results agree with each other closely up to the thickness between one-eighth and one-quarter of the predominant wavelength. Obviously, the thin-bed assumption inherent in equation (III) breaks down at a thickness greater than one-eighth but less than one-quarter of the predominant wavelength. Note that in all the three cases of equal polarity, the modelling results indicate gradual decreases of the peak frequency as the bed thickness increases. This is indeed predicted by equation (III).

For the opposite polarity cases, Model 1A, which is the Widess' case, show good agreement between the modelling and theoretical results. The slight discrepancy between the two curves is probably due to round-off errors in the modelling package. We shall discuss this further later. For models 1B and 1C, the theoretical curves depart from the modelling curves between two and three meters. In equation (III), the behavior of f versus the bed thickness is very much dependent on how close the absolute value of r_1 approaches that of r_2 , due to the factor $(r_1 + r_2)$ in the denominator. Recall that if $r_1 = -r_2$, the value of f is a constant $(\sqrt{3/2}f_o)$ for all thicknesses up to the thin bed limit. Hence, a singularity exists in the behavior of f in equation III as r_1 approaches r_2 . The closer r_1 is to r_2 , the thinner the thickness range will be in which the modelling results can be predicted by equation (III). In our example, $r_1 + r_2 = .0704$, if we had used different values for r_1 and r_2 so that $r_1 + r_2 = 0.5$ for example, the theoretical and modelling curves would probably agree with each other to thicknesses beyond three meters.

PHASE

To study the phase of the reflected composite wavelet, we shall use complex attributes. The reason is two-fold. Firstly, for the purpose of our research, phase means the shape of the wavelet, not its phase spectrum. Since the instantaneous phase and the instantaneous frequency are independent of the reflection amplitude (Taner, 1979), they should reveal waveform changes more distinctly than regular seismic data. Secondly, the use of complex attributes for seismic exploration has not been discussed widely in published literature. While they were initially developed for use in electrical engineering (Gabor, 1946); their potential use for seismic exploration was emphasized by Taner and et al (1977, 1979) and Robertson and Nogami (1984). As a secondary objective, we wish to explore further their properties with respect to seismic exploration. We shall discuss the attributes separately. The reader is assumed to be familiar with the theory of complex attributes, as it will not be discussed here. A good reference on the subject is the paper by Taner (1979).

(a) Instantaneous Amplitude

Figure 5 shows the instantaneous amplitude plots for the six models. For the unequal polarity models, the only difference in the thickness of interest is the magnitude of the amplitude. Thus, given only one of the three plots, 5a, 5b or 5c, one cannot differentiate which case it is.

For the equal polarity case, there are clear differences in the shape of the envelope and the timing of the peak amplitude. For the equal strength case, the peak starts splitting into two distinct peaks at a thickness slightly under one-quarter of the predominant wavelength. But the symmetry of the character remains throughout the whole model. But for cases 5e and 5f, there is no splitting, but the peak shifts up in time in 5e and down in 5f in the thickness of interest. Thus, based on the instantaneous amplitude alone, one could possibly differentiate between the three cases of equal polarity. Given the model as shown in Figure 1, Figures 2d, 2e and 2f, these instantaneous amplitude results are perhaps to be expected. Below one-eighth of the predominant wavelength, there is not much difference among the three amplitude attributes. Note that for the unequal polarity cases, the amplitude increases as thickness, and vice versa for the equal polarity cases for the thickness of interest. Furthermore, tuning at one-quarter of the predominant wavelength as reported by Robertson and Nogami (1984) is observed on all cases.

(b) Instantaneous Phase

Figure 6 shows the instantaneous phase plots for the six models. As pointed out by Taner (1979) and Robertson et al (1984), the instantaneous phase is a very effective tool for delineating discontinuities, faults, pinchouts, angularities and events with different dip attitudes. This is mainly due to the fact that the instantaneous phase is independent of the amplitude. Hence, one would expect that any subtle waveform changes will be clearly outlined by the instantaneous phase.

Figures 6d, 6e and 6f are the phase plots for the equal polarity models. For these three models, there is no detectable phase change until the thickness thickens to about a quarter of the predominant wavelength. This implies that either there is no change in the wavelet shape for smaller thicknesses, or else the change is too subtle to be detected.

For the unequal polarity models, the results are somewhat dubious. Firstly, there are problems for the first few traces, particularly in models 1B and 1C. At present, we do not fully understand the cause, but we are investigating the problem and hopefully will resolve it soon. Secondly, there seems to be no phase change in any of the three models until the thickness is about one-half of the predominant wavelength. This appears to contradict Widess' conclusion of the composite wavelet changing to the shape of the derivative of the input wavelet at the thickness equal to one-eighth of the predominant wavelength. A most likely explanation is that any phase change in these models are too subtle to be detected until the thickness is about one-half of the predominant wavelength. But why so subtle? We will not comment further on the reason until we test it out with more models.

(c) Instantaneous Frequency

Since the instantaneous frequency is the derivative of the instantaneous phase, the comments for the latter are applicable to the former. Figures 7d, 7e, 7f are the instantaneous frequency plots for the equal polarity cases. Frequency tuning is observed at about the thickness equal to one-quarter of the predominant wavelength while the frequency pattern is symmetrical in model 1D, it is shifted downwards in 1E and upwards in 1F.

For the unequal polarity models shown in Figures 7a, 7b and 7c, frequency tuning as reported by Robertson and Nogami (1984) is not observed at the thickness equal to one-eighth of the predominant wavelength. As mentioned in the previous section, our results are somewhat dubious, and needs further investigation.

DISCUSSION

Based on the behavior of either the absolute maximum amplitude or the peak frequency, the modelling results indicate that we can differentiate between the equal polarity cases from the unequal polarity cases in the thickness of interest. In Figures 3 and 4, the absolute maximum amplitude and the peak frequency are plotted as a function of the bed thickness. Agreement between the theoretical predicted results and the modelling results are generally good except for model 1B and 1C. Note the absolute maximum amplitude in equation (I) and the peak frequency in equation (III) are also functions of the reflection coefficients r_1 and r_2 . How well the theoretical predicted values agree with the modelling results would probably depend on the values of r_1 and r_2 . For example, in equation (III), the larger the value ($r_1 + r_2$) is the less 'singular' the fraction becomes, and the theoretical values would likely agree with the modelling results for a range of thickness larger than those shown in Figures 3b, 3c, 4b and 4c. Thus, one should also study equations (I) and (III) as a function of r_1 and r_2 .

However, based on the absolute maximum and the peak frequency data, it would be difficult to differentiate among the three cases of equal polarity since they behave similarly as a function of thickness. Nevertheless, measuring the peak to trough ratio might help to differentiate them, as indicated in Figures 3 and 4. The same is true for the three cases of unequal polarity.

For the phase, we need to investigate several problems as mentioned earlier. The attribute plots for the equal polarity cases appear to be in order, but the ones for the unequal polarity cases are not. Nevertheless, an interesting observation is that for the equal polarity cases, there are more differences in the symmetry of the patterns. For example, model 1D shows complete symmetry for all the attributes, while model 1G and 1F show skewed symmetry in the attribute plots. But for the unequal polarity cases, they all exhibit similar symmetry in the thickness of interest.

CONCLUSION

Based on the modelling results, one can conclude that for the equal polarity models, the maximum absolute amplitude in the thickness of interest decreases non-linearly with thickness. In particular, the behavior is very close to being a quadratic function below one-eighth of the predominant wavelength, as indicated by the good match between the modelling and theoretical results. Their peak frequencies also decrease quadratically as a function of thickness.

For the unequal polarity cases, the maximum absolute amplitude in the thickness of interest increases with thickness, the behavior being linear for model 1A. For models 1B and 1C, the functional dependence, i.e. whether it is linear or quadratic, is probably also a function of how different r_1 and r_2 are. The peak frequency for models 1B and 1C first increases and then decreases with thickness. For model 1A, the peak frequency is $\sqrt{3/2}$ times the input peak frequency. Furthermore, as discussed in Appendix B, Widess' conclusion of the reflected composite wavelet changing to the derivative of the input wavelet at one-eighth of the predominant wavelength is verified quantitatively in an indirect manner.

FUTURE WORK

In real seismic data, vertical incidence may only be a good approximation for short spread lengths and deep targets. For long spread lengths and shallow targets, conclusions from the study of vertical incidence may not be applicable. Therefore, the second step will be to extend the work to offset-dependent modelling.

For many areas in Southern Alberta, many reflections from Cretaceous formations are composite reflection of several thin layers. Results from studying two-termed reflectivity series may not be applicable to three-termed or more reflectivity series. Hence, the third step is to extend our investigation into the properties of a wavelet which is comprised of more than two reflections.

REFERENCES

- Berkout, A.J., 1984, Seismic resolution: Handbook of Geophysical Exploration, Section I, v.12, chap.II.
- de Voogd, N. and den Rooijen, H., 1983, Thin-layer response and spectral bandwidth: Geophysics 48, 12-18.
- Gabor, D., 1946, Theory of Communication, part I: J. Inst. Elect. Eng. 93, part III, 429-441.
- Kallweit, R.S. and Wood, L.C., 1982, The limits of zero-phase wavelets: Geophysics 47, P.1035-1046.
- Koefoed, O. and de Voogd, N., 1980, The linear properties of thin layers, with an application to synthetic seismograms over coal seams: Geophysics 45, 1254-1268.
- Lange, J.N. and Almoghrabi, 1988, Lithology discrimination for thin layers using wavelet signal parameters: Geophysics 53, 1512-1519.
- Neidell, N.S. and Poggliagliolmi, E., 1977, Stratigraphic modelling and interpretation - Geophysical principles and techniques: AAPG memoir 26, 389-416.
- Ricker, N., 1953, Wavelet contraction, wavelet expansion, and the control of seismic resolution: Geophysics 18, 769-792.
- Robertson, J.D. and Nogami, H.H., 1984, Complex seismic trace analysis of thin beds: Geophysics 49, 344-352.
- Taner, M.T. and Sheriff, R.E., 1977, Applications of Amplitude, Frequency and other Attributes to Stratigraphic and Hydrocarbon Determination: AAPG Memoir 26, 301-327.
- Taner, M.T., Koehler, F. and Sheriff, R.E., 1979, Complex seismic trace analysis: Geophysics 44, 1041-1063.
- Widess, M.B., 1973, How thin is a thin bed?: Geophysics 38, 1176-1180.
- _____, 1982, Quantifying resolving power of seismic systems: Geophysics 47, 1160-1173.

Appendix A

Let us derive equation (I). Our approach will follow that of Widess' method (1973). To the first order of approximation, the central portion of the Ricker zero phase wavelet can be approximated by a sine wave whose maximum amplitude is A_i . Choosing the centre of the thin bed as the zero time reference, we have

$$\phi = \frac{A_r}{A_i} = r_1 \cos\left(t + \frac{b}{V}\right) \frac{2\pi}{T_d} + r_2 \cos\left(t - \frac{b}{V}\right) \frac{2\pi}{T_d} \quad (\text{A-a})$$

where A_r = amplitude of reflected composite wavelet

b = thickness of the thin bed

V = P-wave velocity within the thin bed

T_d = predominant period of the wave

r_1 = reflection coefficient of upper interface

r_2 = reflection coefficient of lower interface

$$\therefore \phi = (r_1 + r_2) \cos \frac{2\pi t}{T_d} \cos \frac{2\pi b}{\lambda_d} + (r_2 - r_1) \sin \frac{2\pi t}{T_d} \sin \frac{2\pi b}{\lambda_d}$$

where λ_d = predominant wavelength of the wavelet

Now, we make the thin bed approximation. For sufficiently small b , $\frac{\sin \frac{2\pi b}{\lambda_d}}{\lambda_d} = \frac{2\pi b}{\lambda_d}$ and

$$\cos \frac{2\pi b}{\lambda_d} = 1 - 2 \left(\sin \frac{\pi b}{\lambda_d} \right)^2 = 1 - 2 \left(\frac{\pi b}{\lambda_d} \right)^2$$

$$\therefore \phi = (r_1 + r_2) \left[1 - 2 \left(\frac{\pi b}{\lambda_d} \right)^2 \right] \cos \frac{2\pi t}{T_d} + (r_2 - r_1) \frac{2\pi b}{\lambda_d} \sin \frac{2\pi t}{T_d}$$

$$= M_1 \cos \frac{2\pi t}{T_d} + M_2 \sin \frac{2\pi t}{T_d}$$

$$\text{where } M_1 = (r_1 + r_2) \left[1 - 2 \left(\frac{\pi b}{\lambda_d} \right)^2 \right] \quad \text{and} \quad M_2 = (r_2 - r_1) \frac{2\pi b}{\lambda_d}$$

For absolute maximum ϕ ,

$$\frac{d\phi}{dt} = 0 = -\frac{2\pi}{T_d}M_1 \sin \frac{2\pi t}{T_d} + \frac{2\pi t}{T_d}M_2 \cos \frac{2\pi t}{T_d}$$

$$\therefore \tan \frac{2\pi t}{T_d} = \frac{M_2}{M_1} \quad \text{and} \quad t = \frac{T_d}{2\pi} \tan^{-1} \left(\frac{M_2}{M_1} \right)$$

$$\begin{aligned} \therefore \phi_{\text{abs. max.}} &= M_1 \cos \frac{2\pi}{T_d} \left[\frac{T_d}{2\pi} \tan^{-1} \left(\frac{M_2}{M_1} \right) \right] + M_2 \sin \frac{2\pi}{T_d} \left[\frac{T_d}{2\pi} \tan^{-1} \left(\frac{M_2}{M_1} \right) \right] \\ &= M_1 \frac{M_1}{\sqrt{M_1^2 + M_2^2}} + M_2 \frac{M_2}{\sqrt{M_1^2 + M_2^2}} = \sqrt{M_1^2 + M_2^2} \end{aligned}$$

$$\therefore \phi_{\text{abs. max.}} = \left\{ (r_1 + r_2)^2 \left[1 - 2 \left(\frac{\pi b}{\lambda_d} \right)^2 \right]^2 + (r_2 - r_1)^2 \left(\frac{2\pi b}{\lambda_d} \right)^2 \right\}^{1/2}$$

Appendix B

Let us derive equation (III).

The spectrum of a two-termed reflectivity series is

$$X(f) = r_1 e^{2\pi i f \Delta t_1} + r_2 e^{2\pi i f \Delta t_2}$$

where r_1 = reflection coefficient of the first term

r_2 = reflection coefficient of the second term

Δt_1 = two-way traveltime from time zero to first term

Δt_2 = two-way traveltime from time zero to second term

f = frequency

$$\therefore X(f) = [r_1 \cos(2\pi f \Delta t_1) + r_2 \cos(2\pi f \Delta t_2)] + i[r_1 \sin(2\pi f \Delta t_1) + r_2 \sin(2\pi f \Delta t_2)]$$

The corresponding amplitude spectrum is then

$$\begin{aligned}
A(f) &= \sqrt{[r_1 \cos(2\pi f \Delta t_1) + r_2 \cos(2\pi f \Delta t_2)]^2 + [r_1 \sin(2\pi f \Delta t_1) + r_2 \sin(2\pi f \Delta t_2)]^2} \\
&= \sqrt{r_1^2 + r_2^2 + 2r_1 r_2 [\cos(2\pi f \Delta t_1) \cos(2\pi f \Delta t_2) + \sin(2\pi f \Delta t_1) \sin(2\pi f \Delta t_2)]} \\
&= \sqrt{r_1^2 + r_2^2 + 2r_1 r_2 \cos(2\pi f \Delta T)}
\end{aligned}$$

where $\Delta T = \Delta t_2 - \Delta t_1 =$ two-way traveltime in the thin layer.

The amplitude spectrum of a Ricker zero-phase wavelet with peak frequency f_0 is (Ricker, 1953)

$$A_r(f) = \left(\frac{f}{f_0}\right)^2 e^{-\left(\frac{f}{f_0}\right)^2}$$

If $R(f)$ is the amplitude spectrum of the convolution of the two-termed reflectivity series with a Ricker zero-phase wavelet, then

$$\begin{aligned}
R(f) &= A(f) A_r(f) \\
&= \left(\frac{f}{f_0}\right)^2 e^{-\left(\frac{f}{f_0}\right)^2} \sqrt{r_1^2 + r_2^2 + 2r_1 r_2 \cos(2\pi f \Delta T)}
\end{aligned}$$

Taking the first derivative of $R(f)$ with respect to f , we have

$$\begin{aligned}
\frac{dR(f)}{df} &= \left(\frac{f}{f_0}\right)^2 e^{-\left(\frac{f}{f_0}\right)^2} \frac{-4\pi r_1 r_2 \Delta T \sin(2\pi f \Delta T)}{2\sqrt{r_1^2 + r_2^2 + 2r_1 r_2 \cos(2\pi f \Delta T)}} \\
&\quad + \sqrt{r_1^2 + r_2^2 + 2r_1 r_2 \cos(2\pi f \Delta T)} \left[2\left(\frac{f}{f_0}\right) \frac{1}{f_0} e^{-\left(\frac{f}{f_0}\right)^2} + \left(\frac{f}{f_0}\right)^2 \left(-2\frac{f}{f_0}\right) \frac{1}{f_0} e^{-\left(\frac{f}{f_0}\right)^2} \right]
\end{aligned}$$

For peak frequency, $\frac{dR(f)}{df} = 0$. Setting $\frac{dR(f)}{df} = 0$ and simplifying, we have

$$\frac{f_p}{f_0} \left[2r_1 r_2 \pi \Delta T \sin(2\pi f_p \Delta T) \right] = \left[r_1^2 + r_2^2 + 2r_1 r_2 \cos(2\pi f_p \Delta T) \right] \left[\frac{2}{f_0} - 2\left(\frac{f_p}{f_0}\right)^2 \frac{1}{f_0} \right]$$

where f_p = the peak frequency .

$$\therefore f_p \left[r_1 r_2 \pi \Delta T \sin(2\pi f_p \Delta T) \right] = \left[r_1^2 + r_2^2 + 2r_1 r_2 \cos(2\pi f_p \Delta T) \right] \left[1 - \left(\frac{f_p}{f_0} \right)^2 \right] \quad (\text{B-a})$$

The above expression is an exact expression relating the peak frequency of a wavelet which is the convoluted product of a two-termed reflectivity series with a zero-phase Ricker wavelet to the time separation of the two reflection spikes, namely, to the thickness of the bed.

We now make the thin bed approximation. For sufficiently small ΔT ,

$$\sin(2\pi f_p \Delta T) \approx 2\pi f_p \Delta T, \quad \text{and} \quad \cos(2\pi f_p \Delta T) \approx 1$$

$$\therefore f_p r_1 r_2 \pi \Delta T (2\pi f_p \Delta T) \approx (r_1^2 + r_2^2 + 2r_1 r_2) \left[1 - \left(\frac{f_p}{f_0} \right)^2 \right]$$

$$(2r_1 r_2 \pi^2 \Delta T^2) f_p^2 = k \left[1 - \left(\frac{f_p}{f_0} \right)^2 \right] \quad \text{where } k = r_1^2 + r_2^2 + 2r_1 r_2 = (r_1 + r_2)^2$$

$$\therefore f_p^2 = \left[\frac{k f_0^2}{2r_1 r_2 \pi^2 \Delta T^2 f_0^2 + k} \right]$$

$$f_p = f_0 \left[\frac{k}{2\pi^2 \Delta T^2 r_1 r_2 f_0^2 + k} \right]^{1/2}$$

$$= f_0 \left[1 + \frac{2\pi^2 \Delta T^2 f_0^2 r_1 r_2}{k} \right]^{-1/2}$$

$$\approx f_0 \left[1 - \frac{\pi^2 \Delta T^2 f_0^2 r_1 r_2}{k} \right] \quad , \text{ to the first order of approximation}$$

The above equation gives the peak frequency as a function of thickness for a thin bed for all cases except when $r_1 = -r_2$. For this special case, $k=0$ and the derived expression for f_0 cannot be applied. However, a different approach of approximation can be taken in equation (B-a).

Putting $r_1 = -r_2$ in equation (B-a), we have

$$\begin{aligned} f_p \left[-r_1^2 \pi \Delta T \sin(2\pi f_p \Delta T) \right] &= \left[2r_1^2 - r_1^2 \cos(2\pi f_p \Delta T) \right] \left[1 - \left(\frac{f_p}{f_0} \right)^2 \right] \\ -f_p \pi \Delta T \sin(2\pi f_p \Delta T) &= 2 \left[1 - \cos(2\pi f_p \Delta T) \right] \left[1 - \left(\frac{f_p}{f_0} \right)^2 \right] \\ &= 2 \left[2 \sin^2(\pi f_p \Delta T) \right] \left[1 - \left(\frac{f_p}{f_0} \right)^2 \right] \end{aligned}$$

Taking the thin bed approximation, where for sufficiently small ΔT , we have

$$\sin(2\pi f_p \Delta T) \approx 2\pi f_p \Delta T, \quad \text{and} \quad \sin^2(\pi f_p \Delta T) \approx (\pi f_p \Delta T)^2$$

$$\therefore 2f_p^2 \pi^2 \Delta T^2 \approx 4\pi^2 f_p^2 \Delta T^2 \left[\left(\frac{f_p}{f_0} \right)^2 - 1 \right]$$

$$\frac{1}{2} = \left[\left(\frac{f_p}{f_0} \right)^2 - 1 \right] \quad \Rightarrow \quad f_p = \sqrt{\frac{3}{2}} f_0$$

This result implies that as the bed thins to below a thickness for which the thin bed approximation is valid, the peak frequency is equal to $\sqrt{\frac{3}{2}} f_0$ and remains constant for that range of thickness. But Lange and Almoghrabi(1988) quantitatively showed that, if we assume that Widess' conclusion of the wavelet changing to its derivative at one-eighth of the predominant wavelength thickness is correct, we will indeed get $\sqrt{\frac{3}{2}} f_0$. Hence, the calculations above indirectly proves the validity of Widess' conclusion.

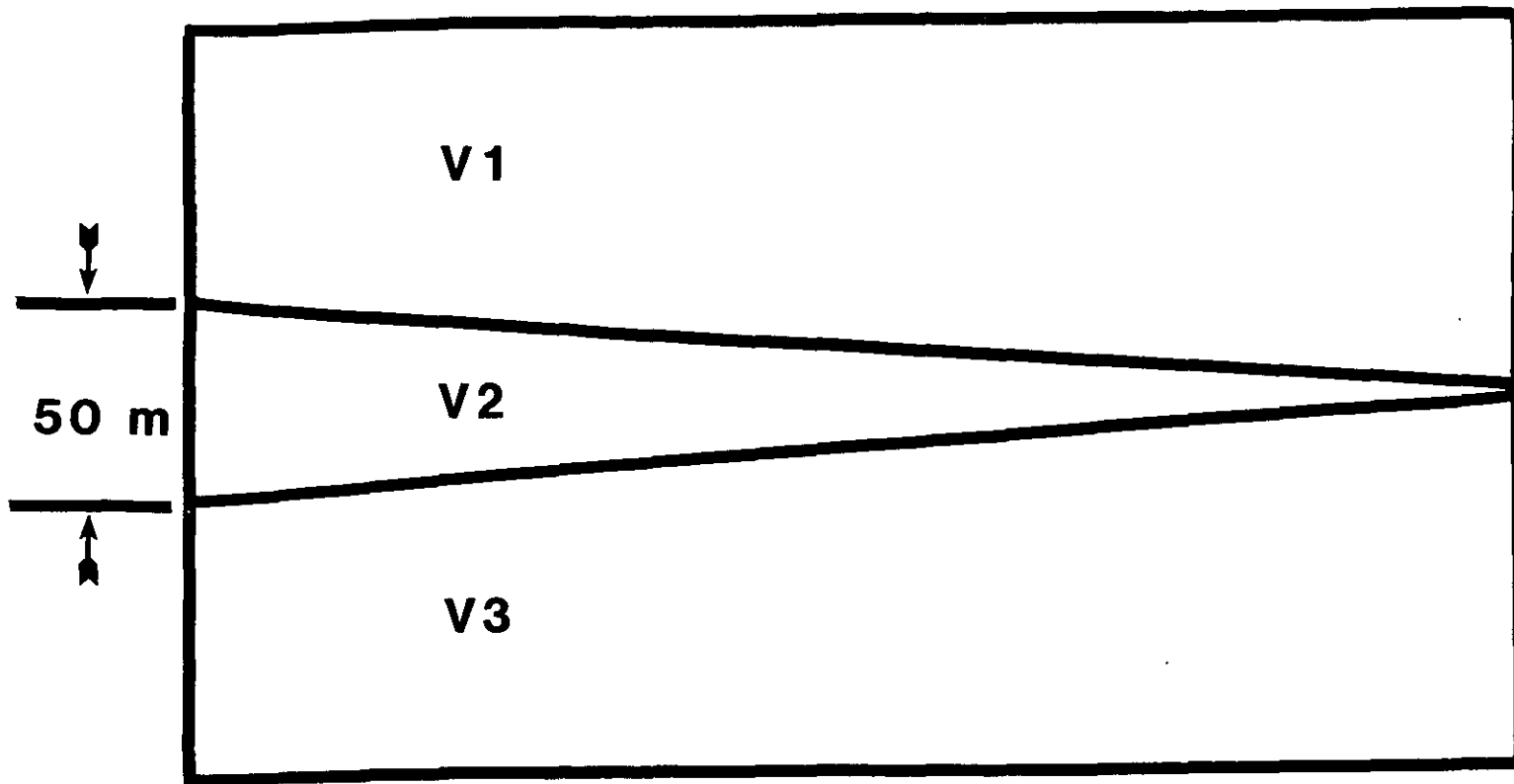


Figure 1. Wedge model

Table 1. Lithology, layer velocities, and layer densities for six models

Model	Lithology Modelled V1(m/s), d(g/cc)	Lithology Modelled V2(m/s), d(g/cc)	Lithology Modelled V3(m/s), d(g/cc)
1A	non-porous sand 4267, 2.502	porous sand 3048, 2.300	non-porous sand 4267, 2.502
1B	silt 3800, 2.430	porous sand 3048, 2.300	non-porous sand 4267, 2.502
1C	non-porous sand 4267, 2.502	porous sand 3048, 2.300	silt 3800, 2.430
1D	porous sand 3048, 2.300	silt 3560, 2.430	non-porous sand 4267, 2.502
1E	porous sand 3048, 2.300	shale 3353, 2.350	non-porous sand 4267, 2.502
1F	porous sand 3048, 2.300	silt 3800, 2.430	non-porous sand 4267, 2.502

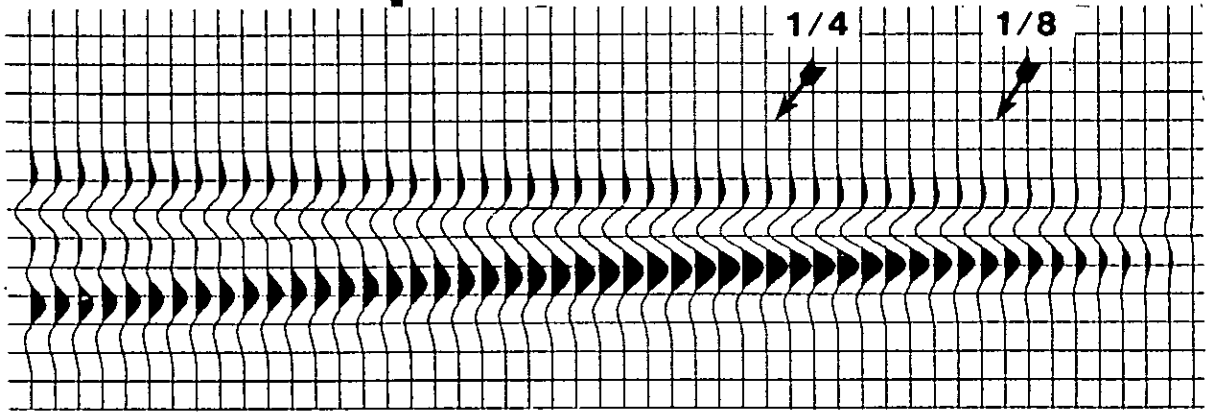
Figure 2

MODEL 1A



410

(a)

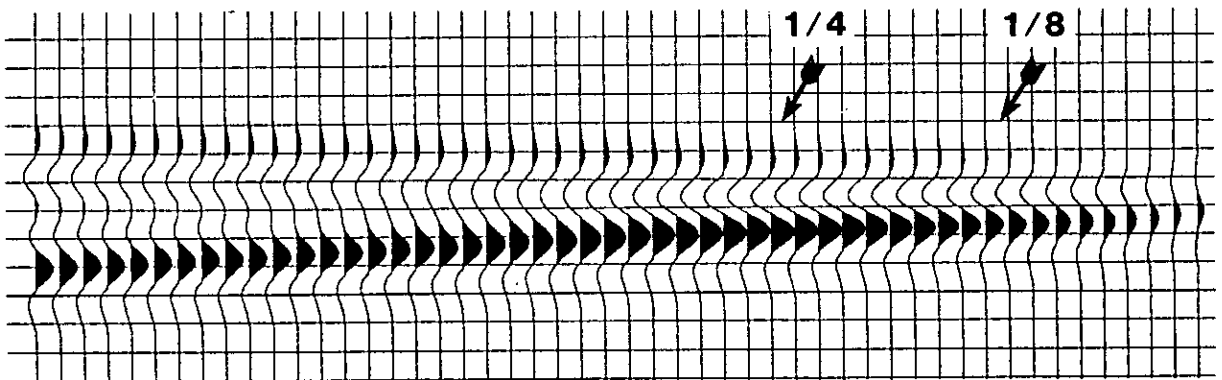


RC are -0.2073 and 0.2073

MODEL 1B



(b)

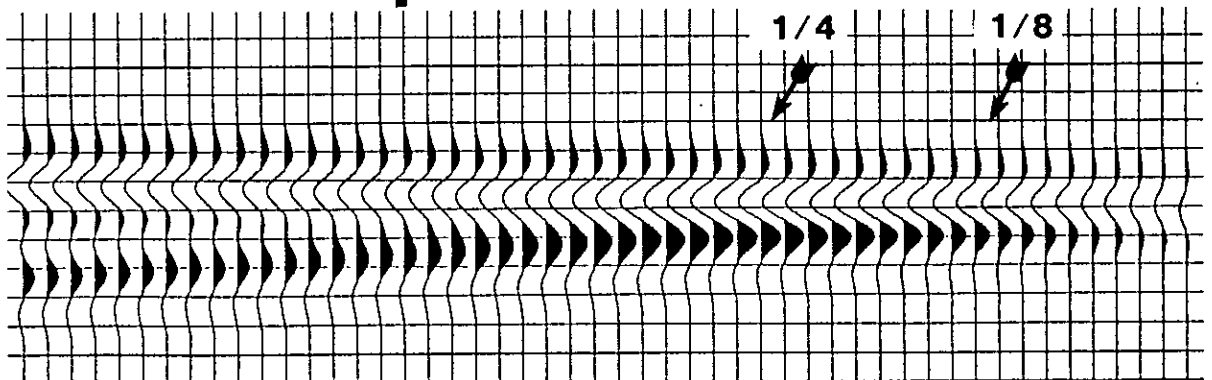


RC are -0.1369 and 0.2073

MODEL 1C



(c)



RC are -0.2073 and 0.1369

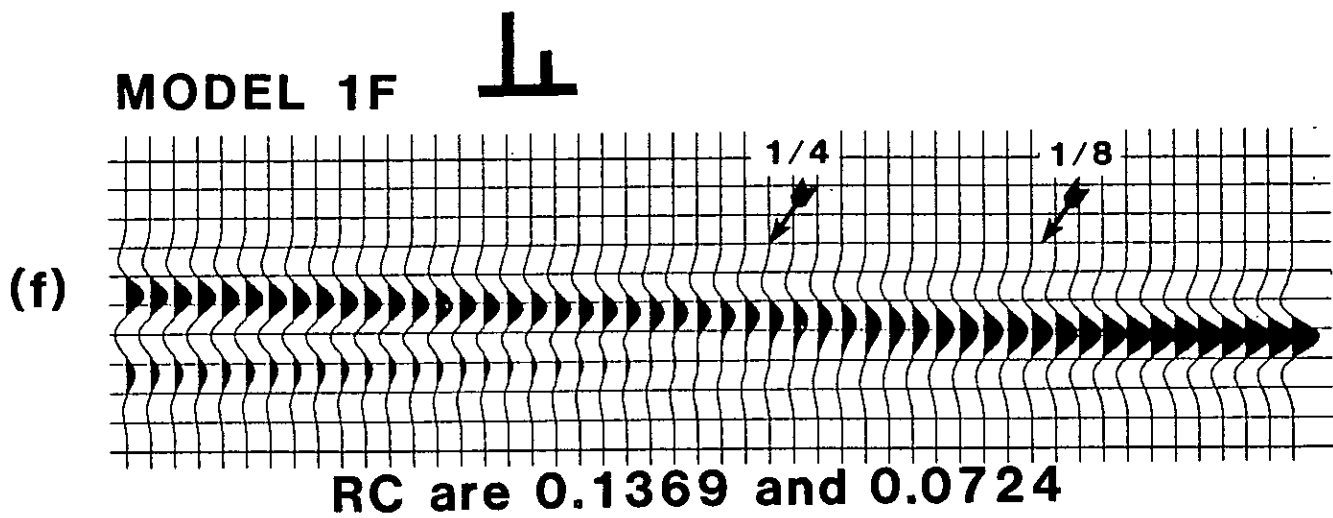
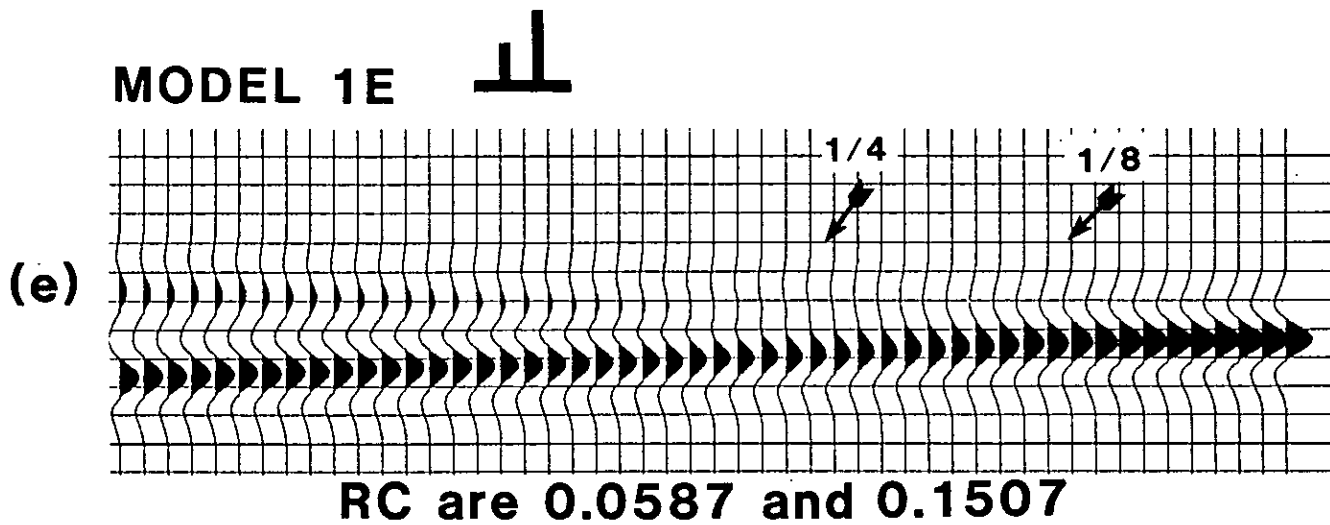
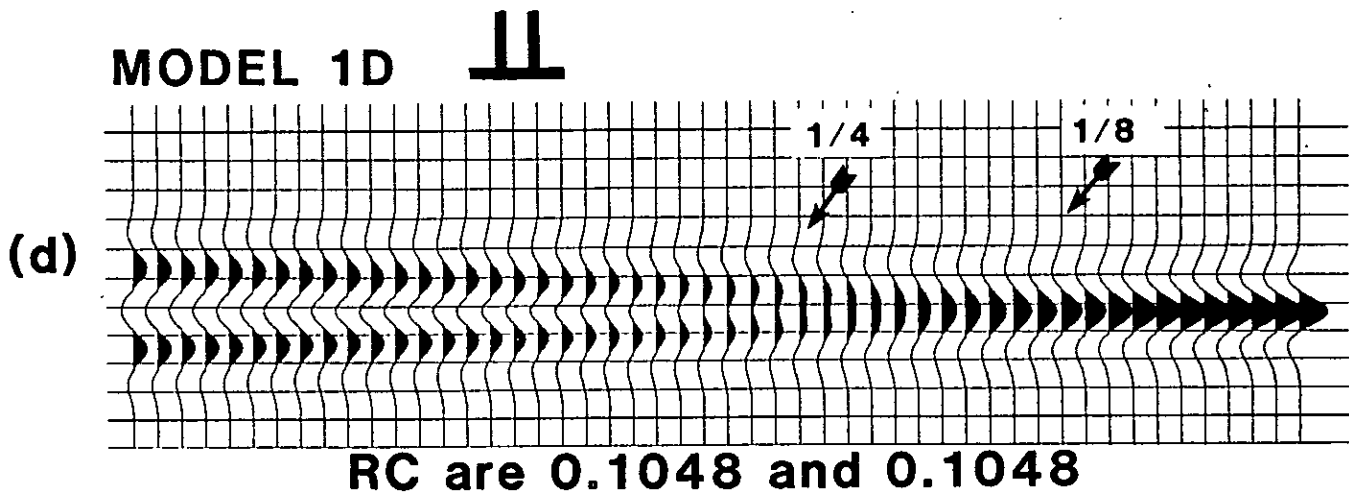



Figure 3a

Model 1A 

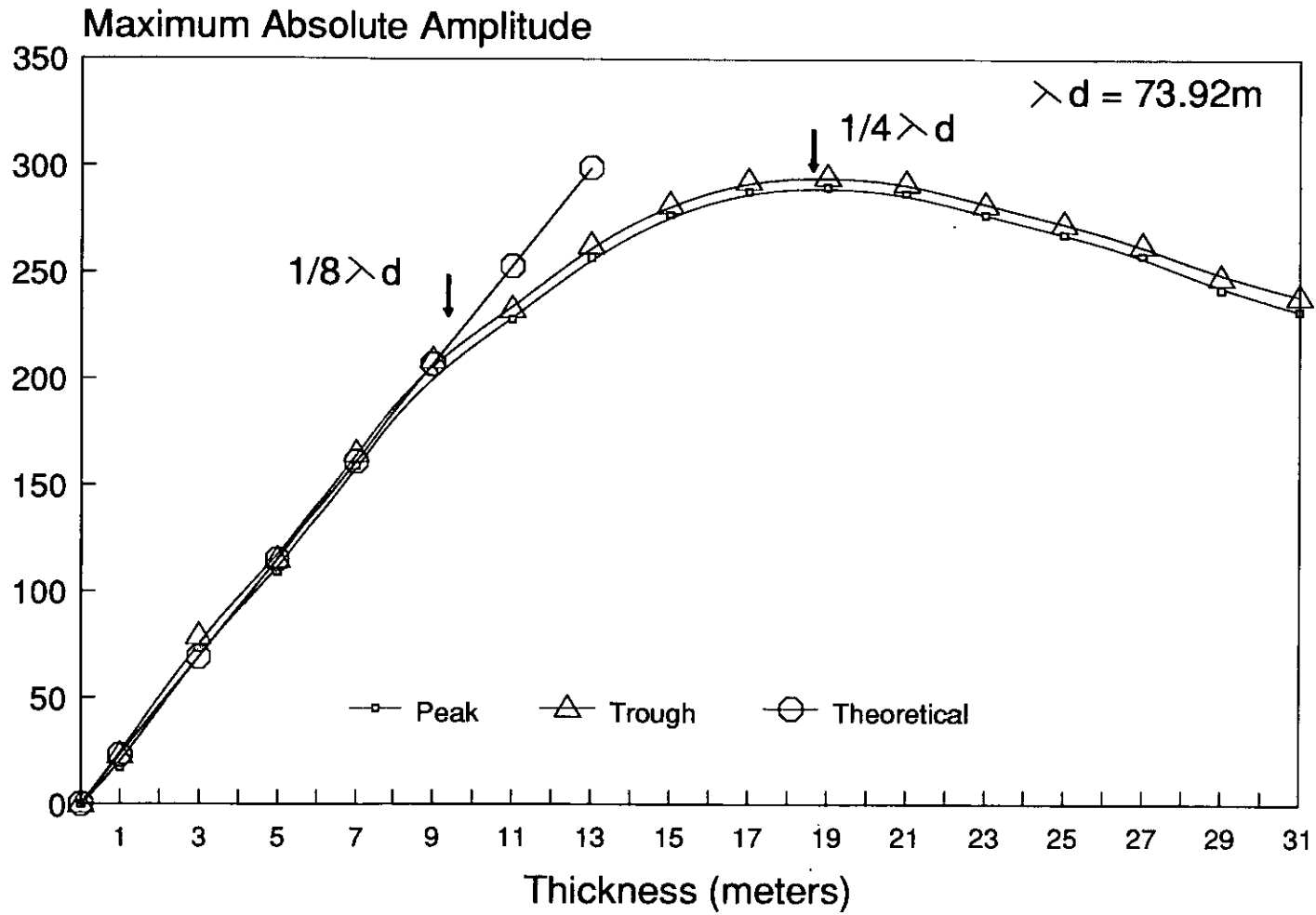


Figure 3b

Model 1B 

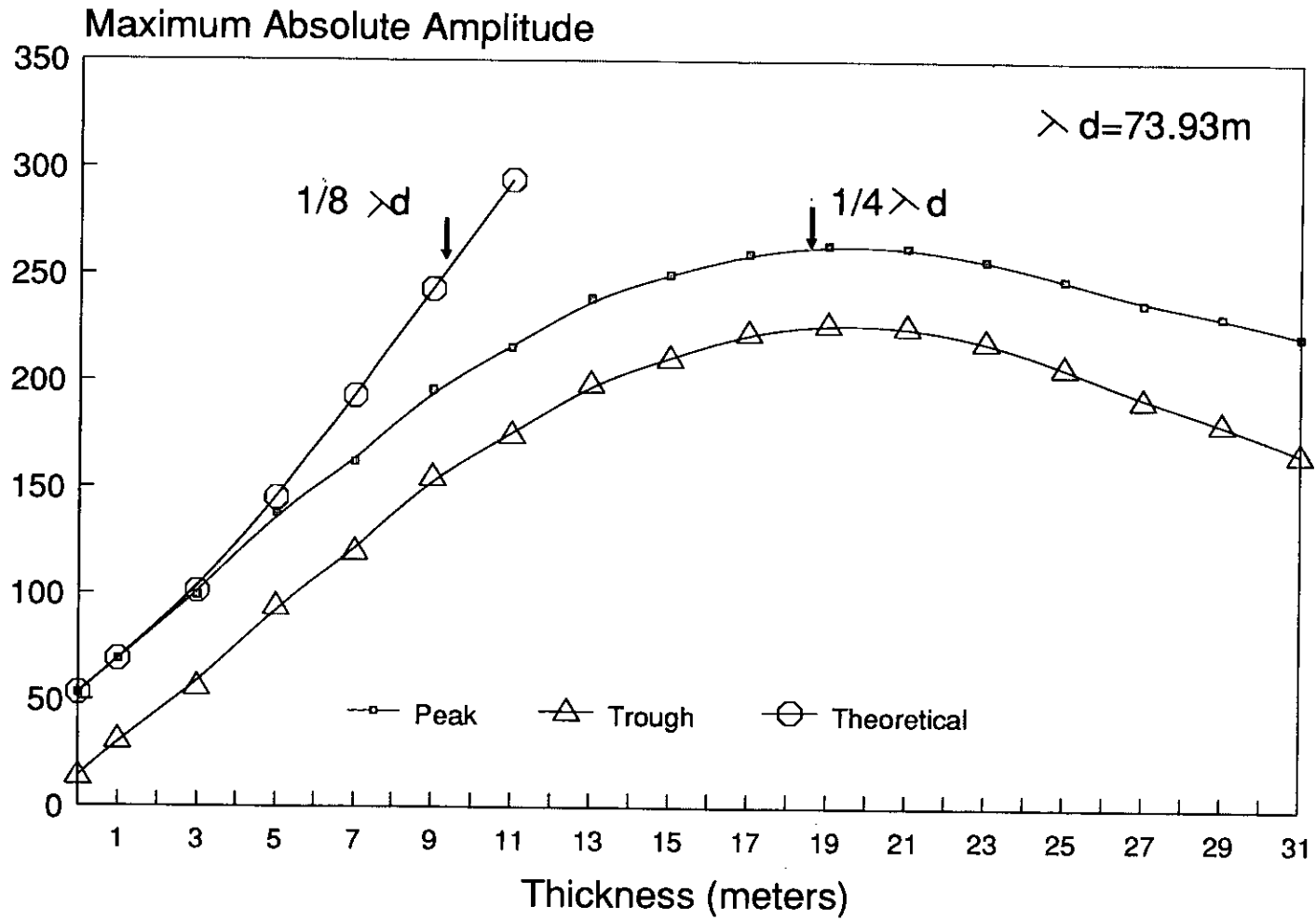
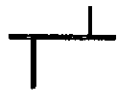


Figure 3c

Model 1C 

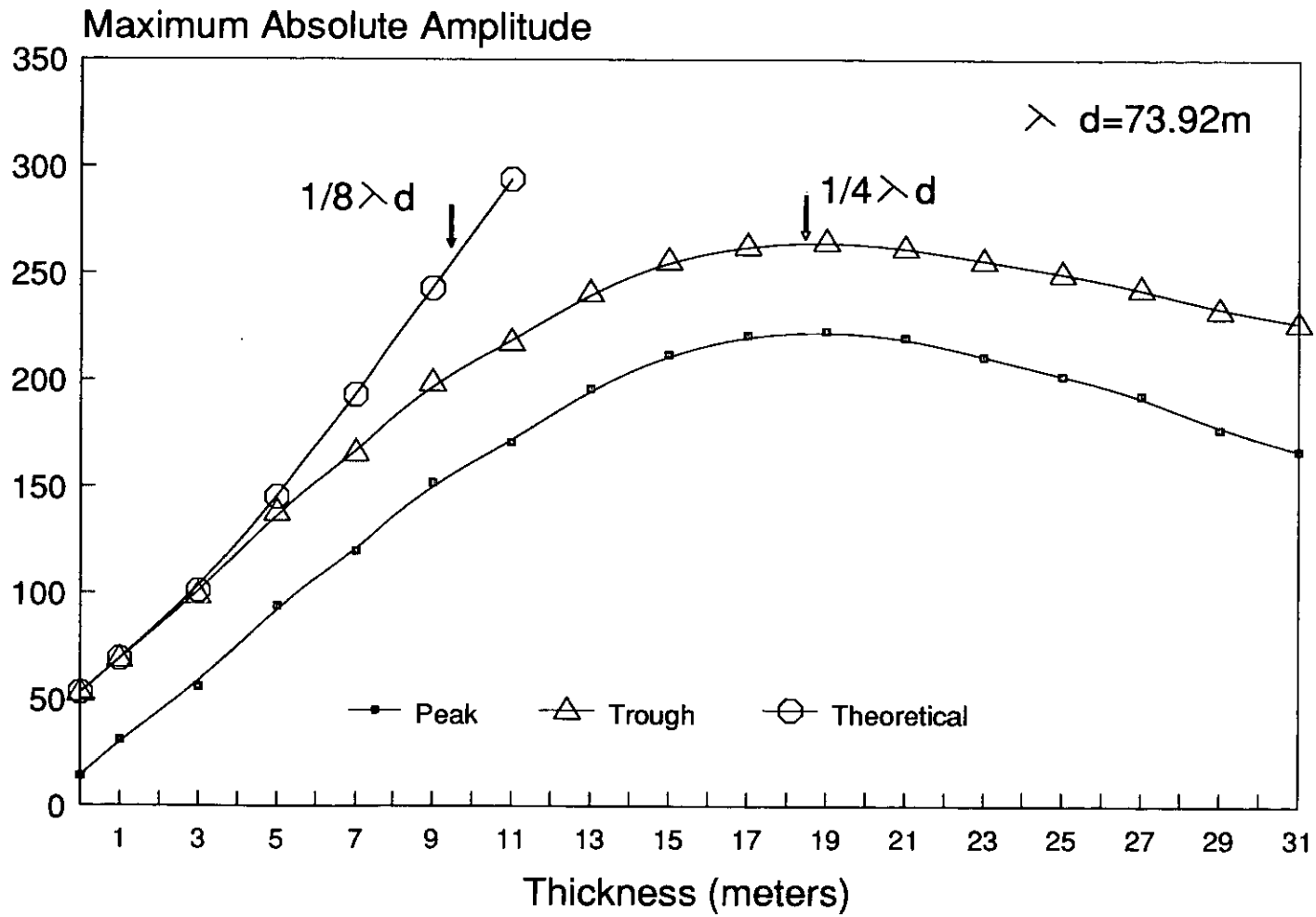


Figure 3d

Model 1D 

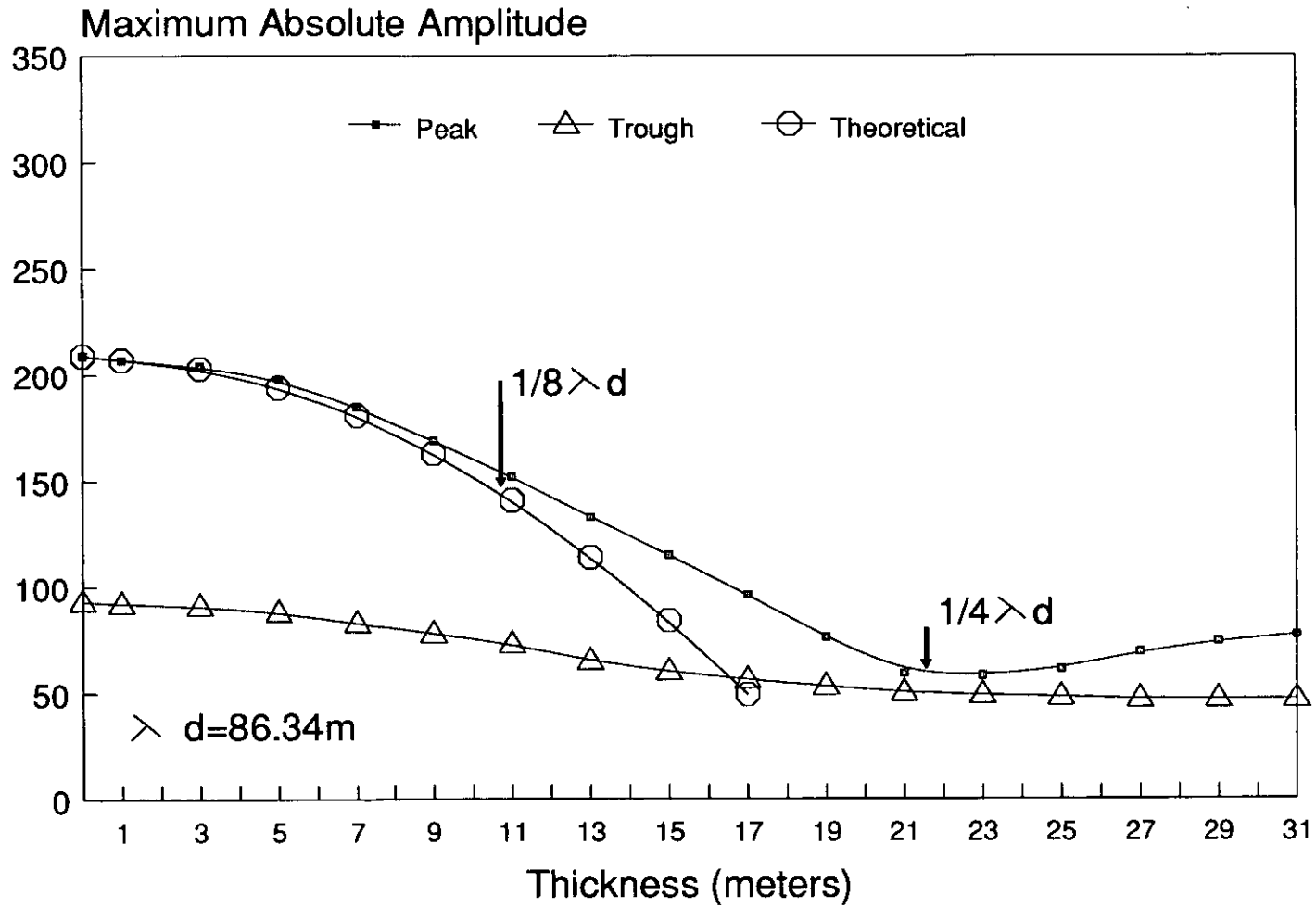


Figure 3e

Model 1E 

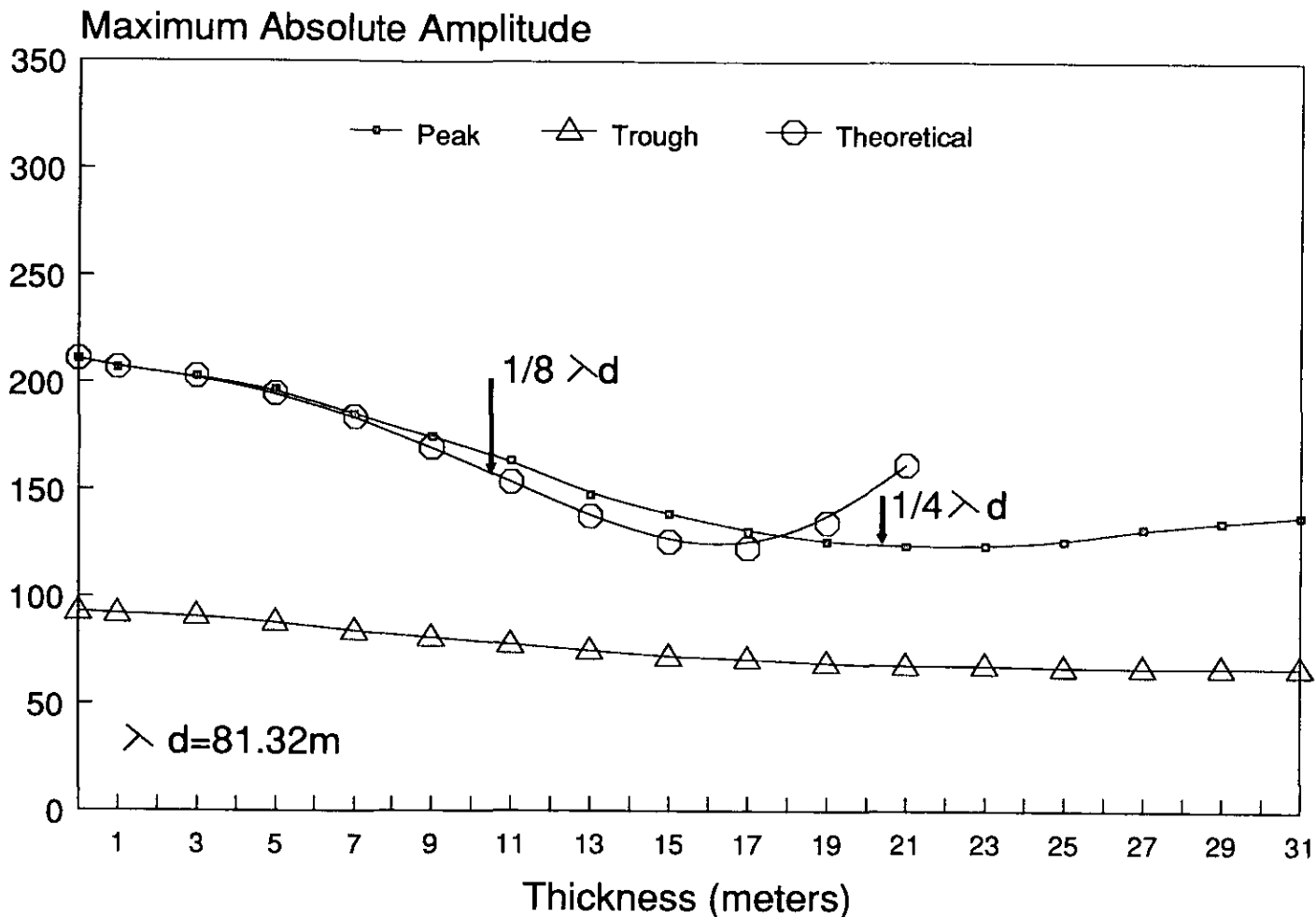



Figure 3f

Model 1F 

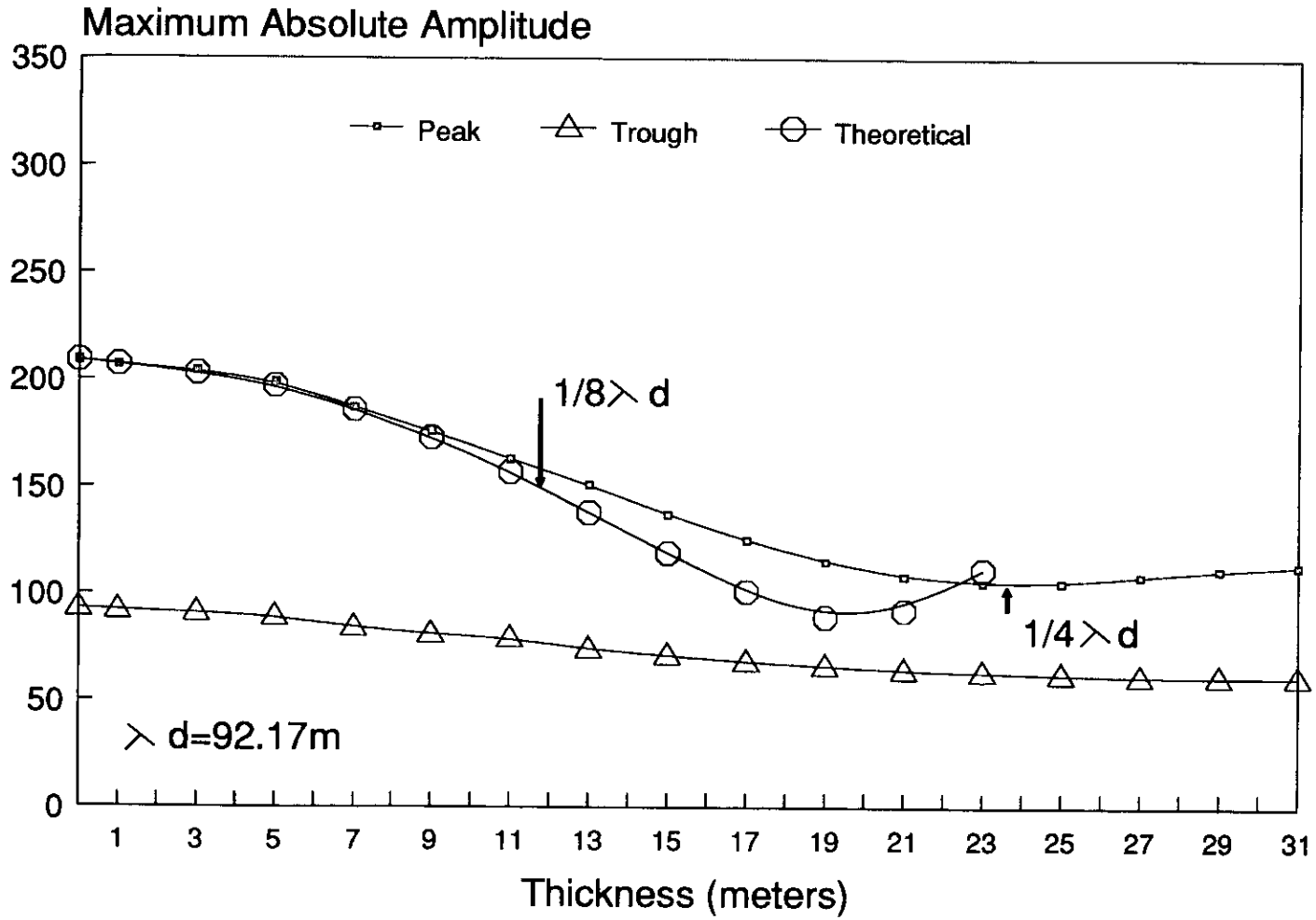


Figure 4a

Model 1A 

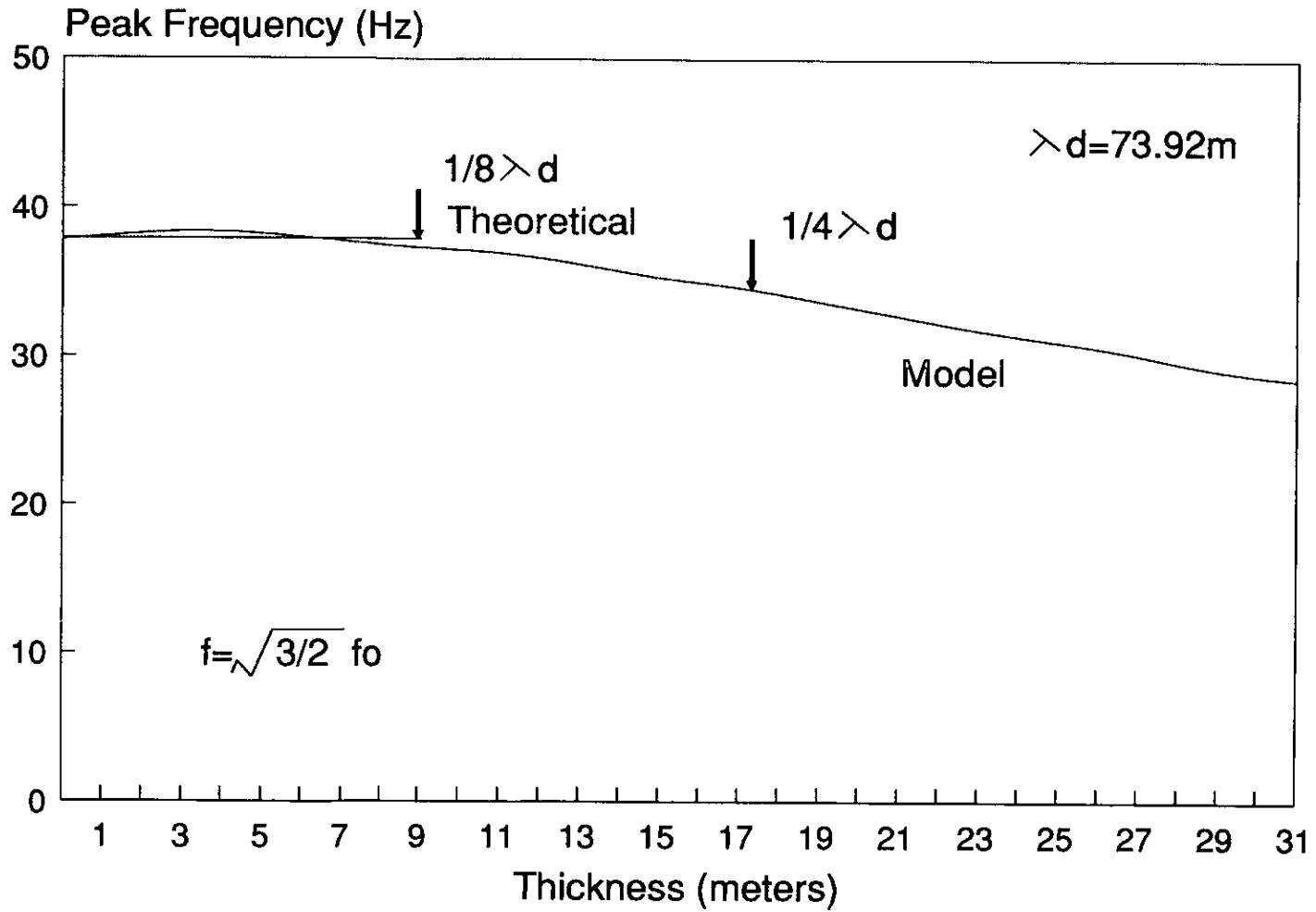


Figure 4b

Model 1B 

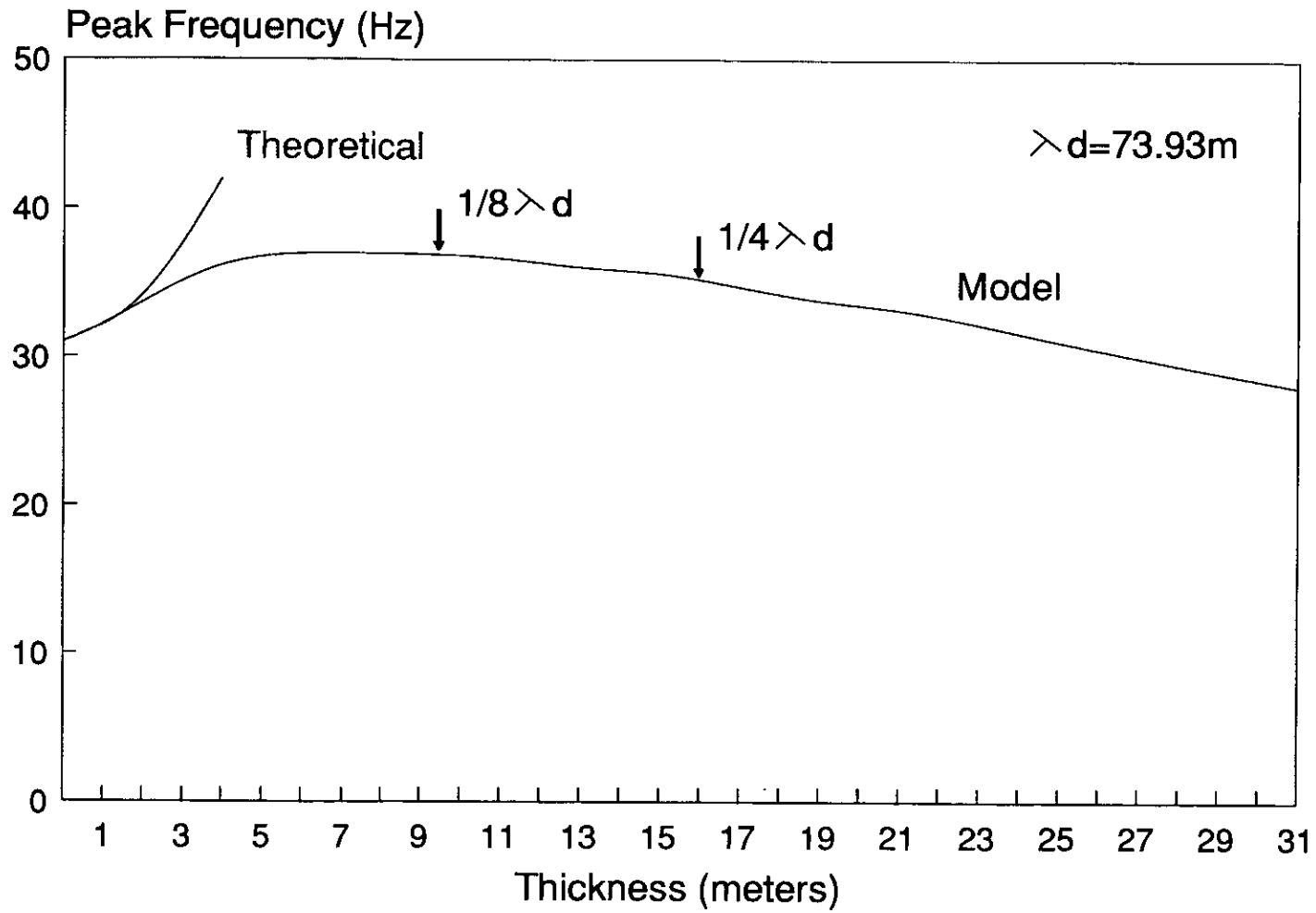



Figure 4c

Model 1C 

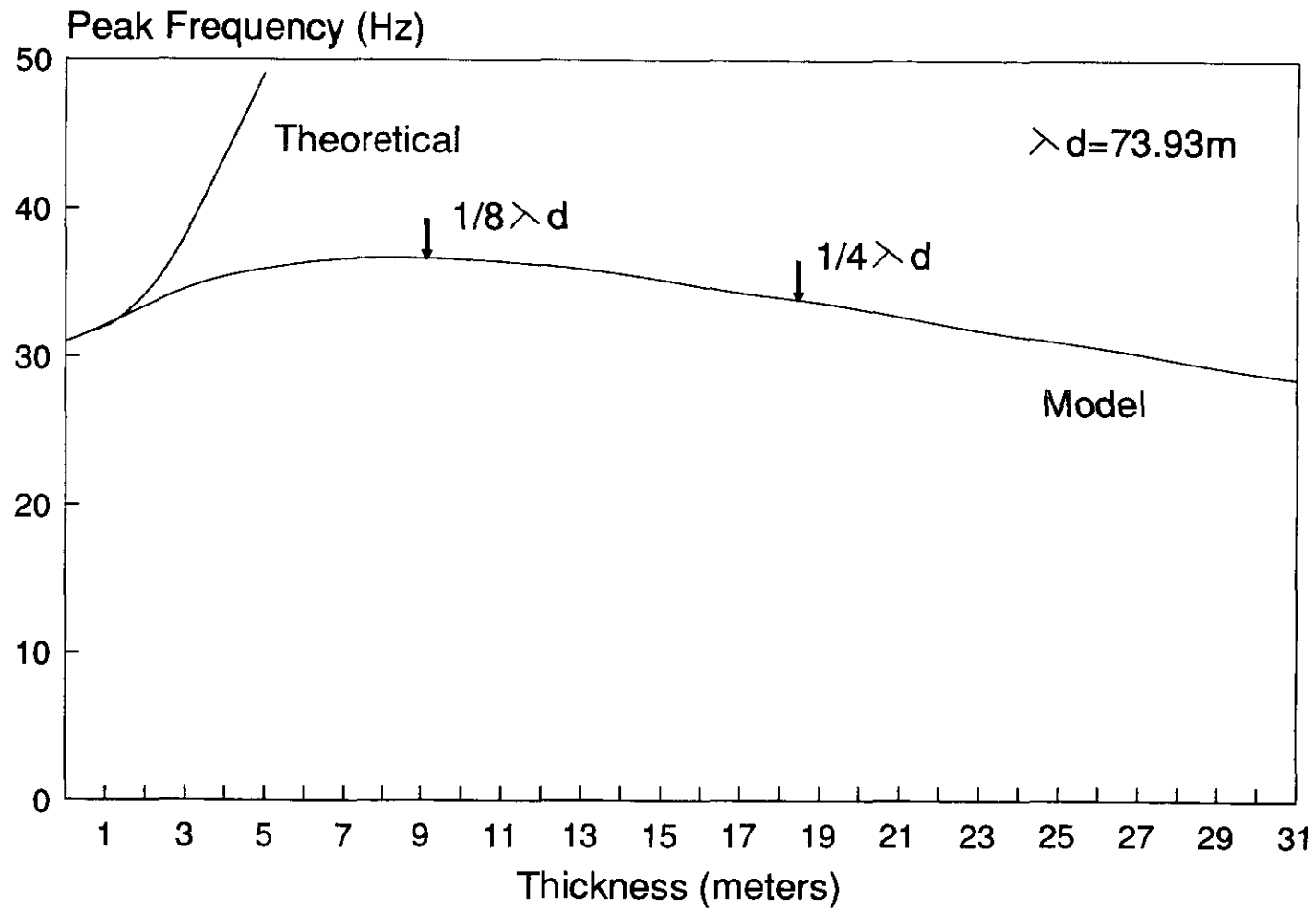


Figure 4d

Model 1D 

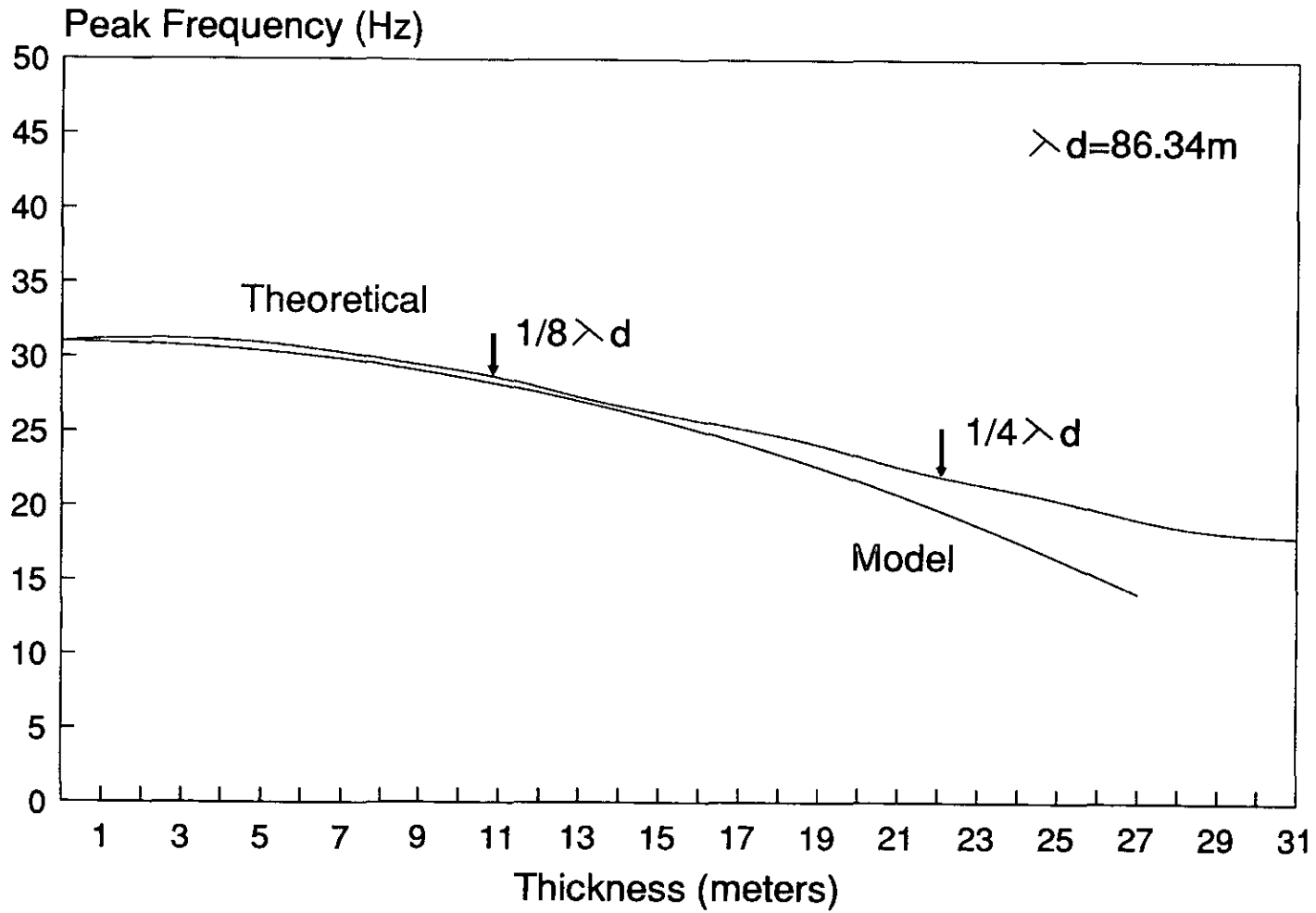


Figure 4e

Model 1E 

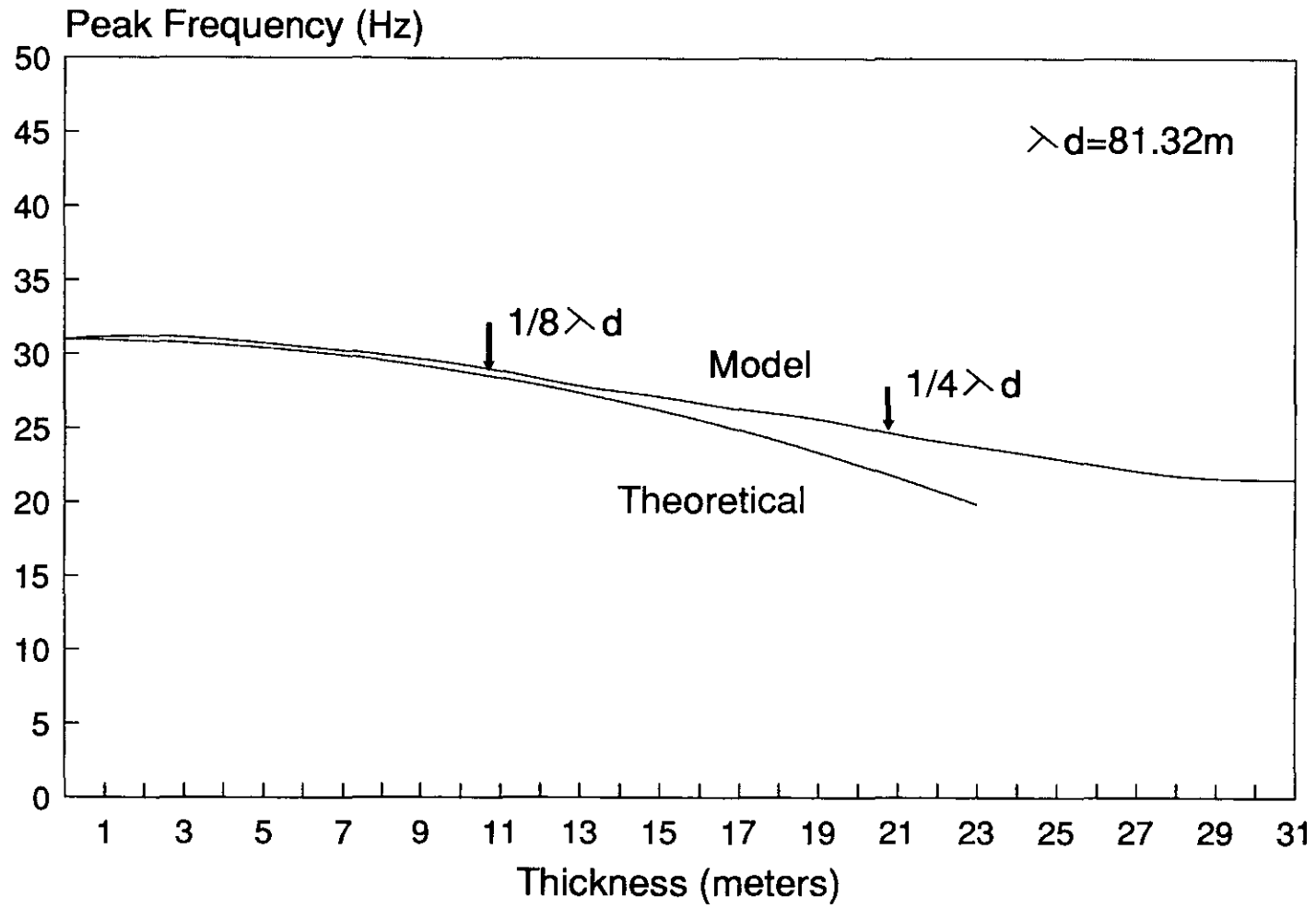


Figure 4f

Model 1F 

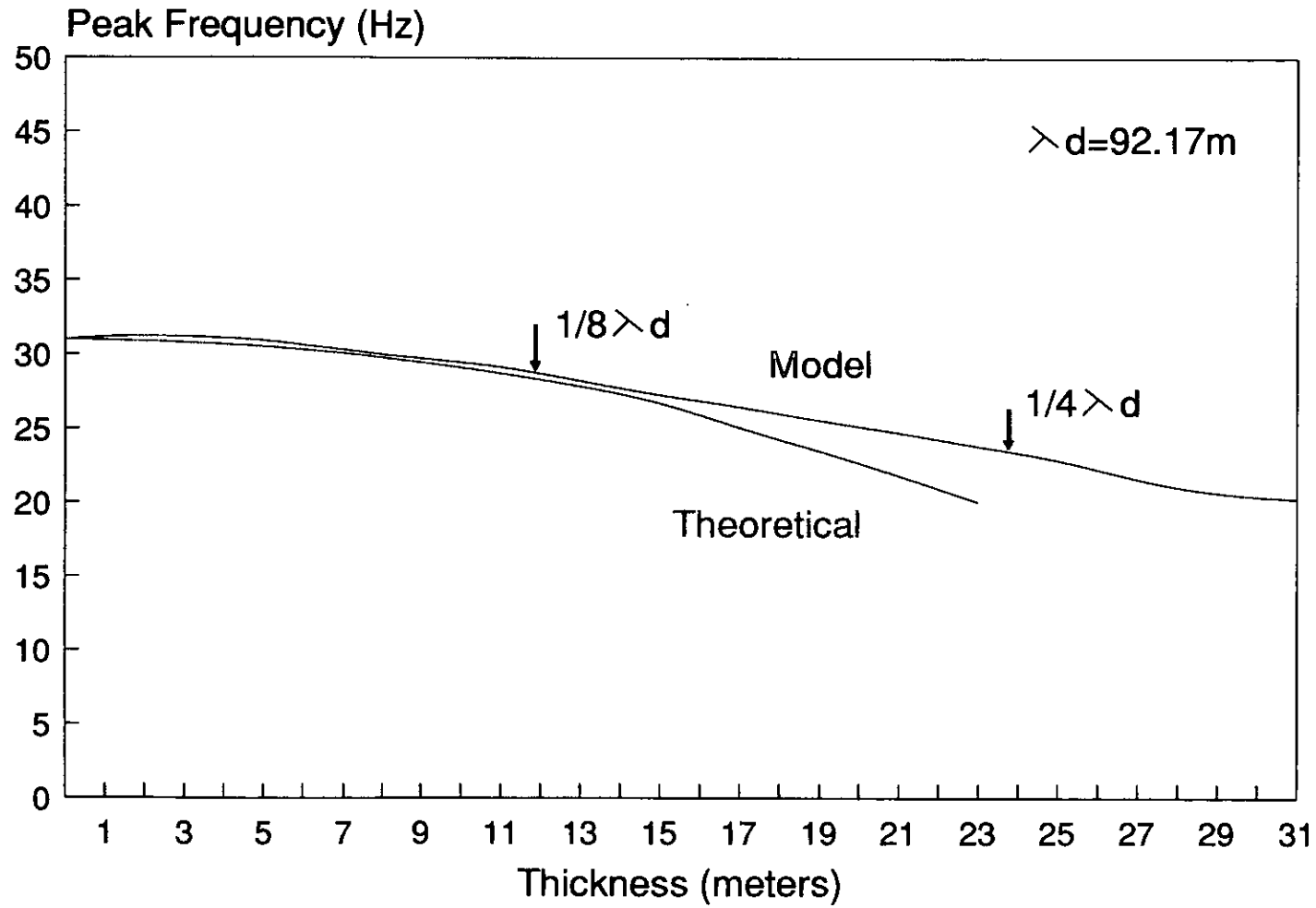


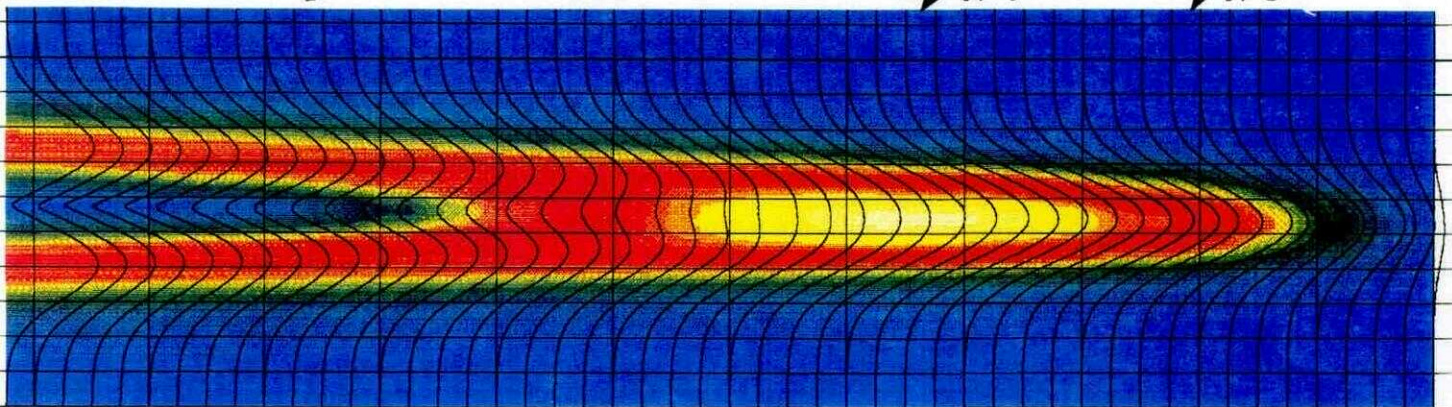
Figure 5

Instantaneous amplitude

(a)



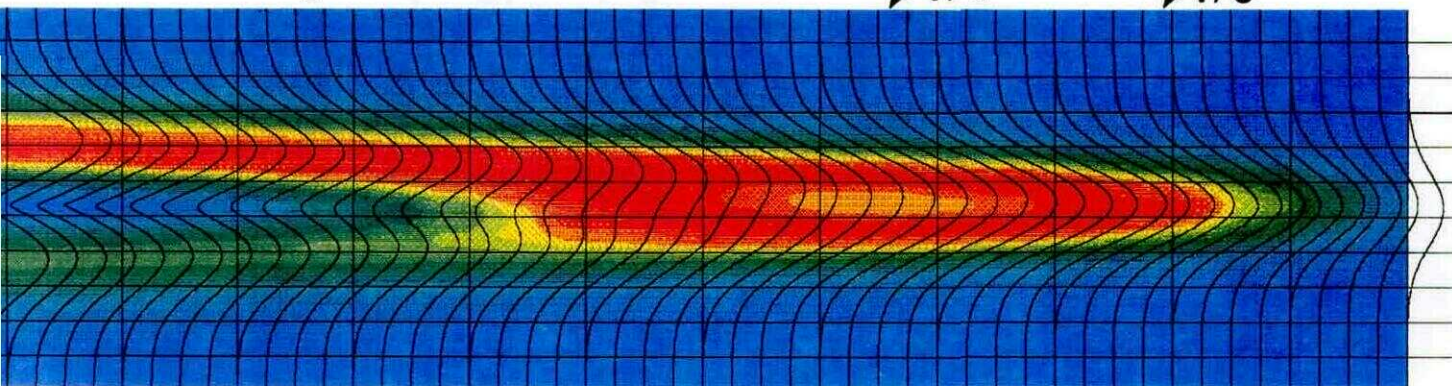
MODEL 1A

 $\frac{1}{4}$ $\frac{1}{8}$ 

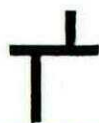
(b)



MODEL 1B

 $\frac{1}{4}$ $\frac{1}{8}$ 

(c)



MODEL 1C

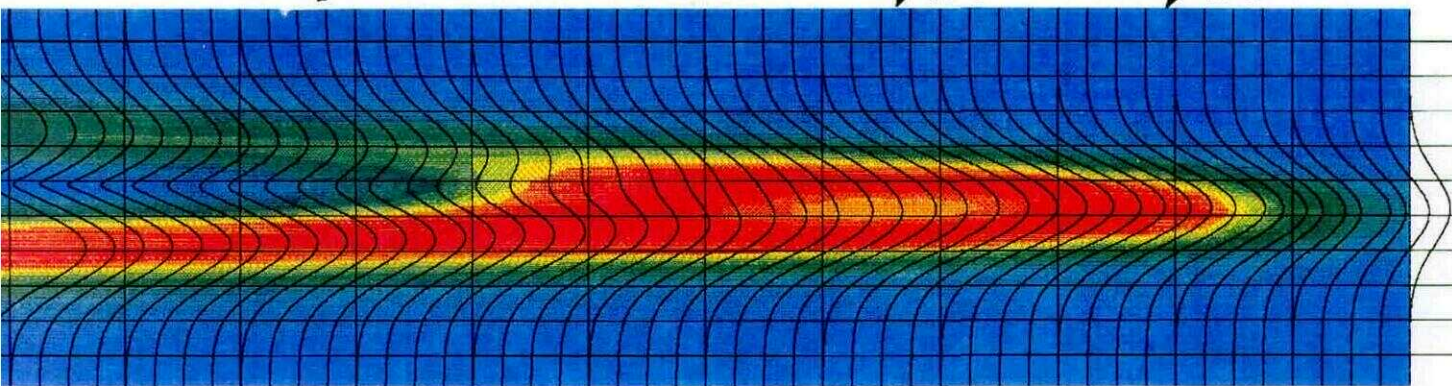
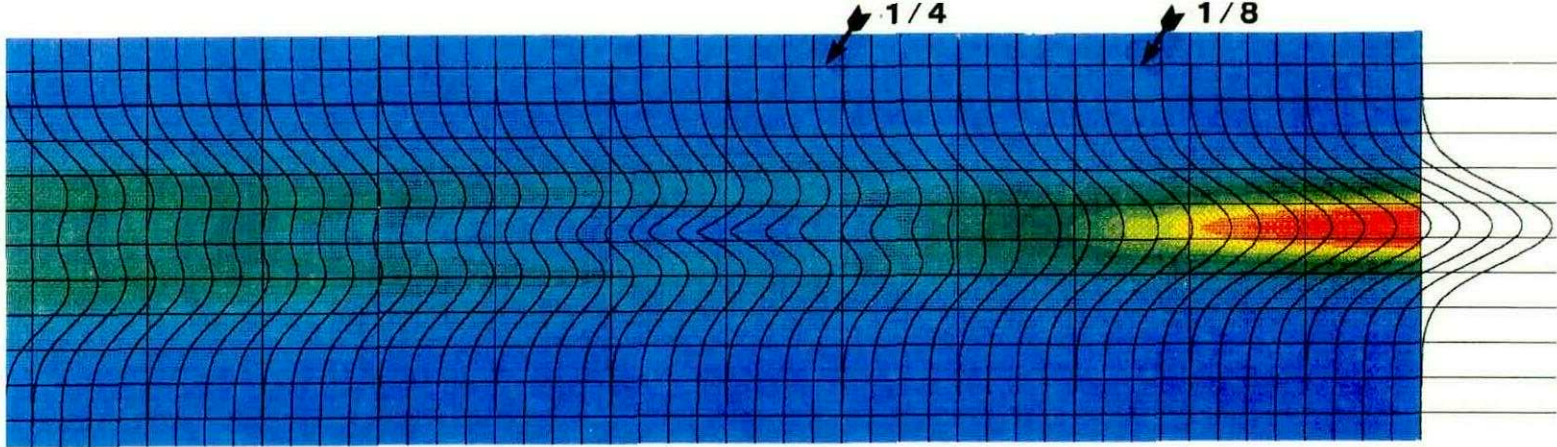
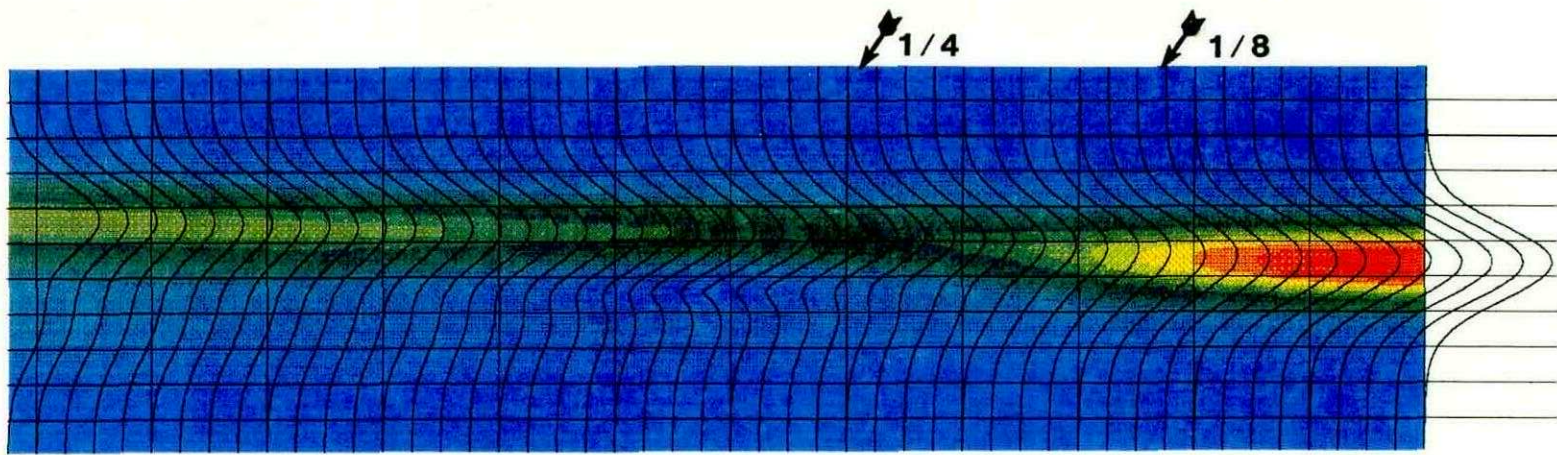
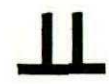
 $\frac{1}{4}$ $\frac{1}{8}$ 

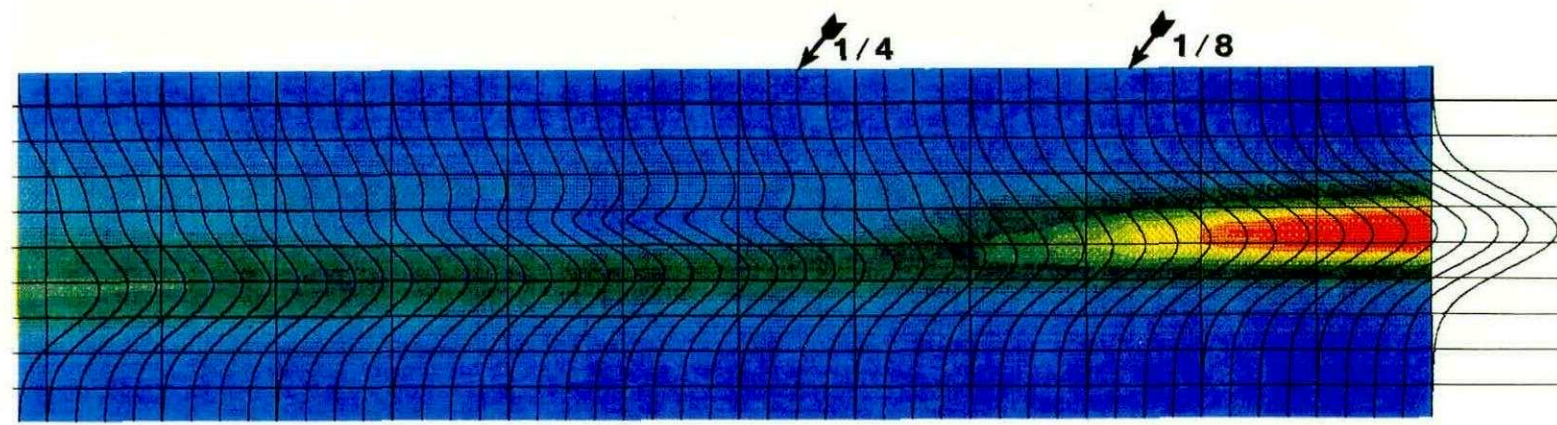
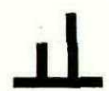
Figure 5



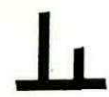
(d)
MODEL 1D



(e)
MODEL 1E



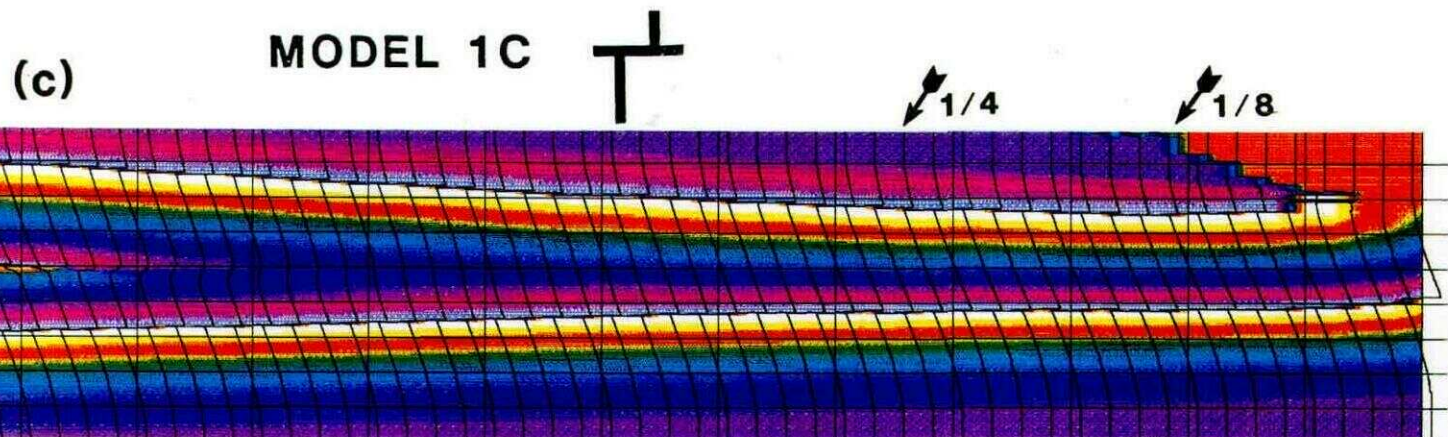
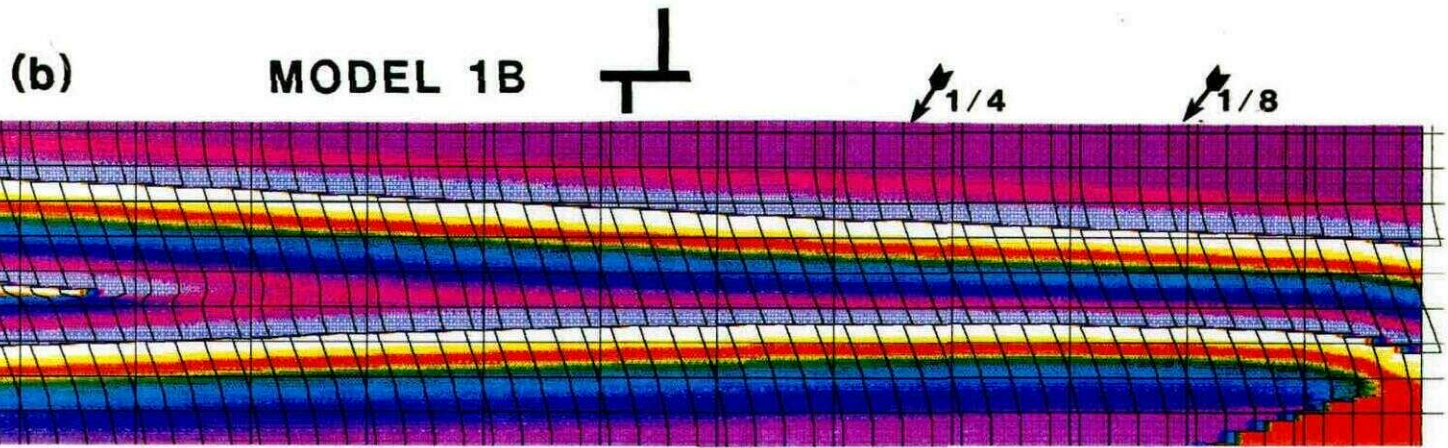
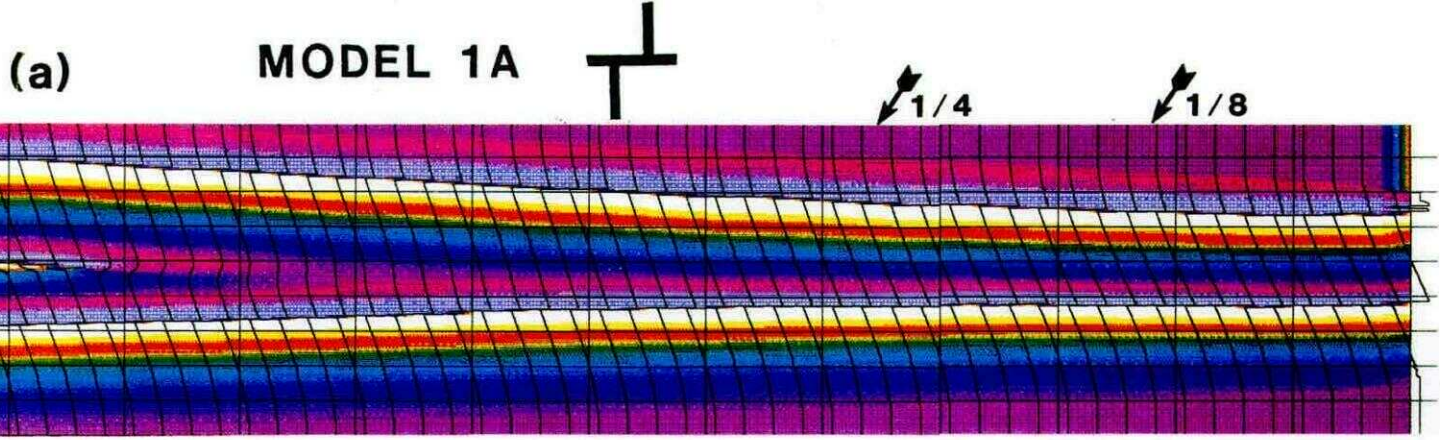
(f)
MODEL 1F



Instantaneous amplitude

Figure 6

Instantaneous phase



427
Figure 6

Instantaneous phase

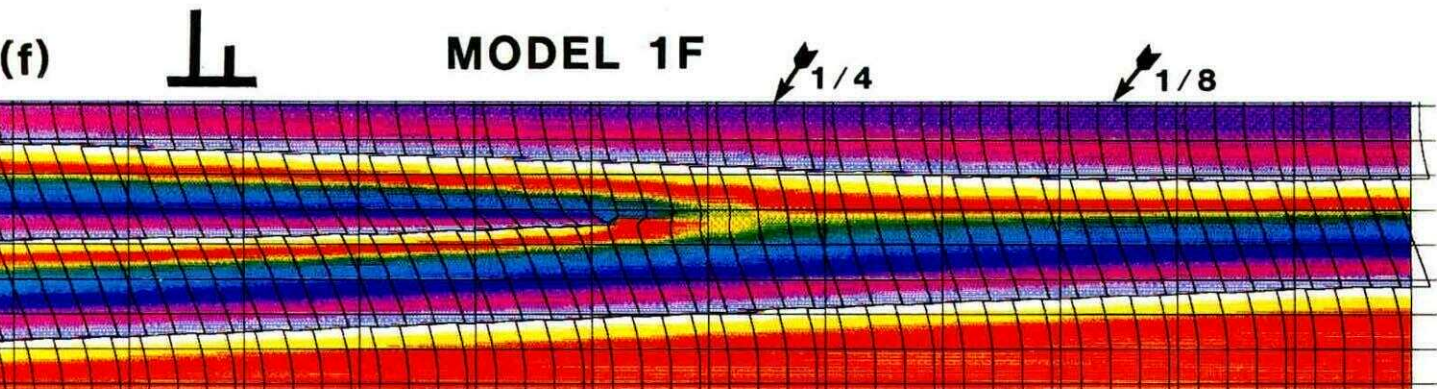
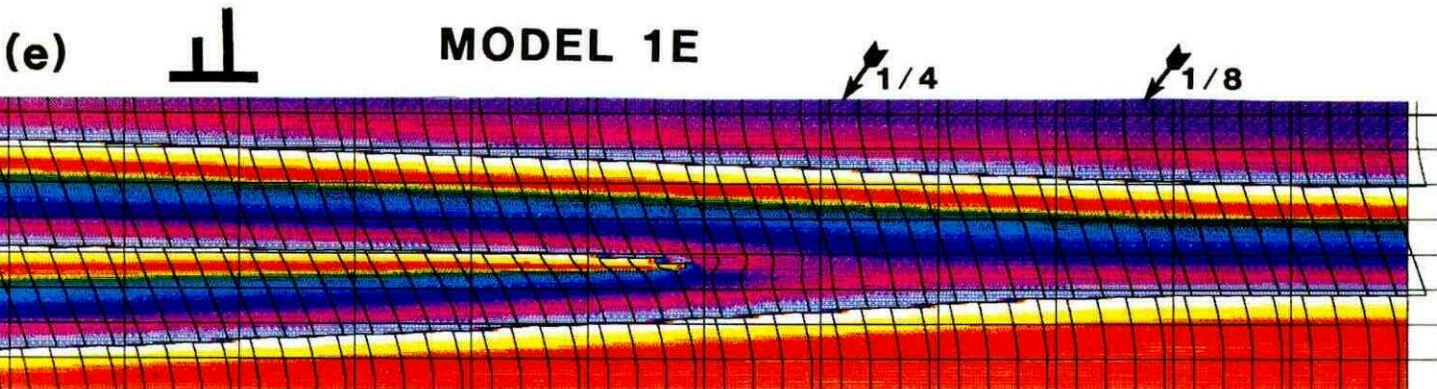
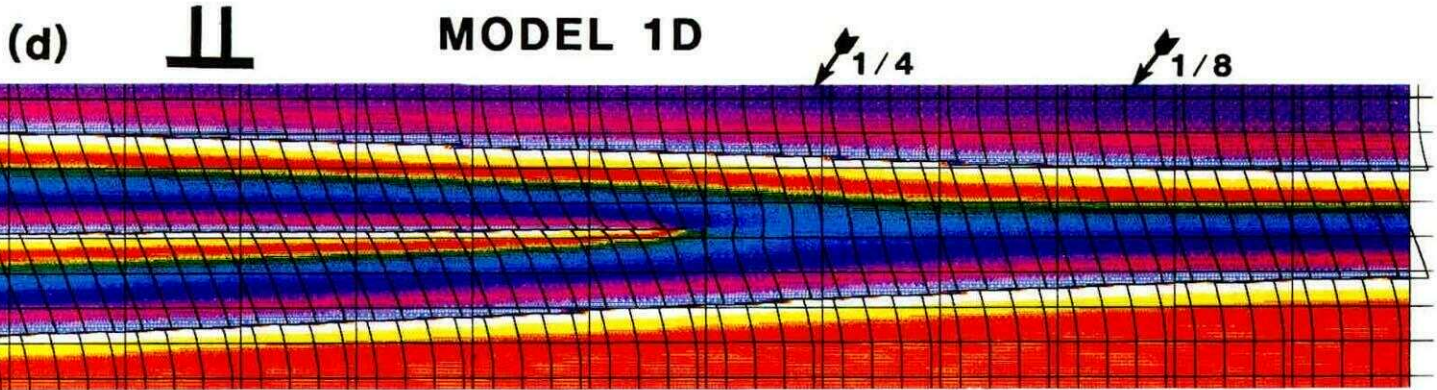
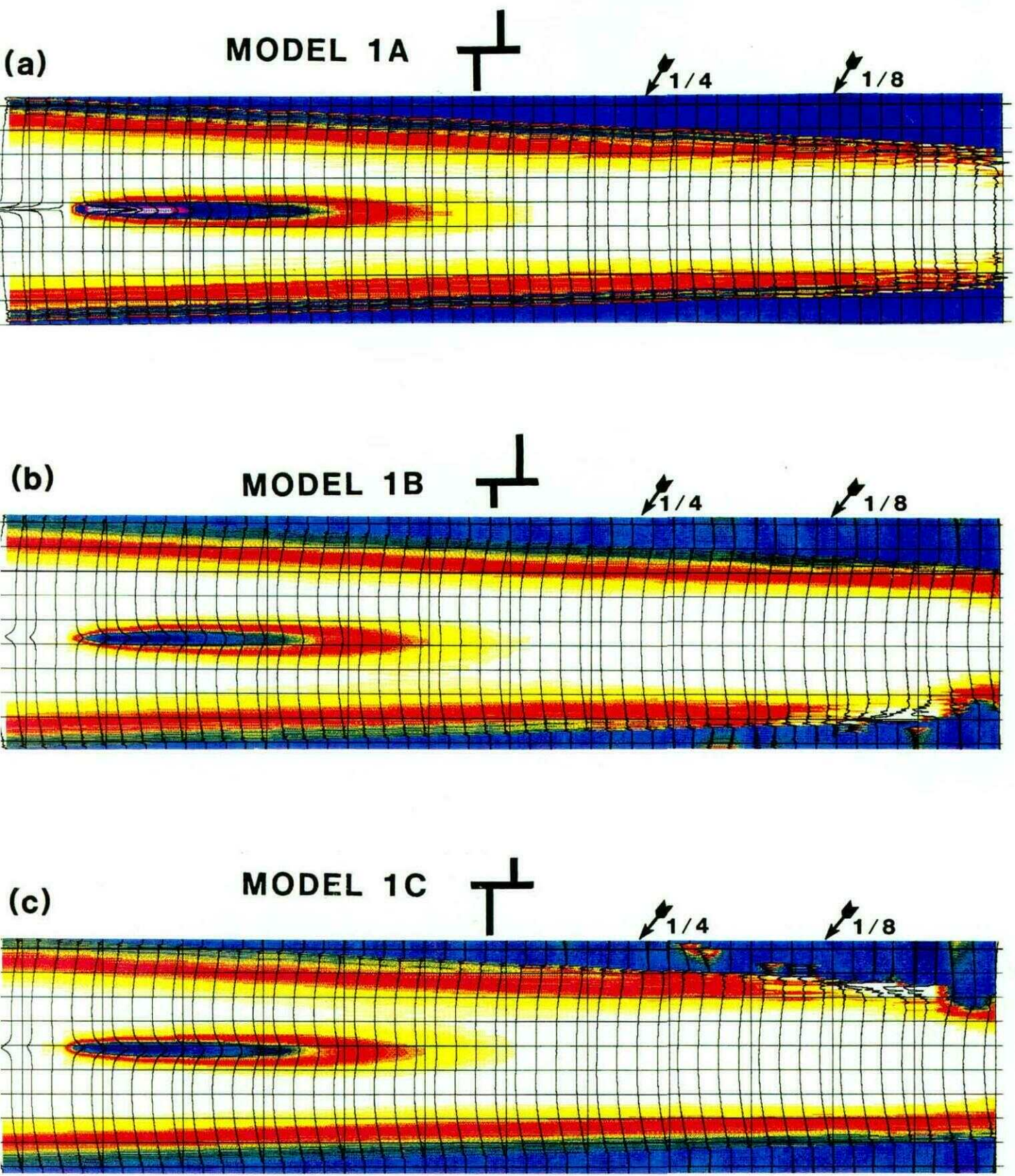


Figure 7

Instantaneous frequency



Instantaneous frequency

